

GEORGIA DOT RESEARCH PROJECT 16-25
FINAL REPORT

**INVESTIGATION AND GUIDELINES FOR MASS
CONCRETE CONSTRUCTION MANAGEMENT**



**OFFICE OF PERFORMANCE-BASED MANAGEMENT
AND RESEARCH
15 KENNEDY DRIVE
FOREST PARK, GA 30297-2534**

1. Report No.: FHWA-GA-19-1625		2. Government Accession No.:		3. Recipient's Catalog No.:	
4. Title and Subtitle: Investigation and Guidelines for Mass Concrete Construction Management			5. Report Date: March 2019		
7. Author(s): Yong Kwon Cho, Russell Gentry, Jason Brown, Lawrence Kahn, and Jisoo Park			6. Performing Organization Code:		
9. Performing Organization Name and Address: School of Civil and Environmental Engineering Georgia Institute of Technology Atlanta, GA 30332-0355			8. Performing Organ. Report No.:		
12. Sponsoring Agency Name and Address: Georgia Department of Transportation Office of Performance-based Management and Research 15 Kennedy Drive Forest Park, GA 30297-2534			10. Work Unit No.:		
			11. Contract or Grant No.: 0015180		
15. Supplementary Notes: Prepared in cooperation with the U.S. Department of Transportation, Federal Highway Administration.			13. Type of Report and Period Covered: Final; July 2016 - March 2019		
			14. Sponsoring Agency Code:		
16. Abstract: The objective of this research is to characterize the heat generation in mass concrete placements typically encountered by GDOT in its construction projects, to create an analytical method for determining the cooling requirements for mass concrete, and to develop a comprehensive guideline for transportation infrastructure applications. This guideline was derived from an extensive review of technical literature and various state DOT's specifications, analytical modeling of heat generation in transportation structures, and laboratory and field research of mass concrete cooling. The guideline can allow GDOT to more efficiently evaluate contractor's proposed mass concrete cooling methods, which would result in improved quality of concrete transportation infrastructures in Georgia.					
17. Key Words: Mass Concrete, Hydration Heat, Thermal Modeling, Analytic Hierarchy Process (AHP)			18. Distribution Statement:		
19. Security Classification (of this report): Unclassified		20. Security Classification (of this page): Unclassified		21. Number of Pages: 46	22. Price:

GDOT Research Project 16-25

Final Report

Investigation and Guidelines for Mass Concrete Construction Management

By

Yong Kwon Cho, Ph.D.
Associate Professor
School of Civil and Environmental Engineering
Georgia Institute of Technology
Telephone: 404-385-2038
Email: yong.cho@ce.gatech.edu

Russell Gentry, Associate Professor
Email: russell.gentry@coa.gatech.edu

Jason Brown, Assistant Professor
Email: jason.brown@coa.gatech.edu

Lawrence Kahn, Professor
Email: lawrence.kahn@ce.gatech.edu

Jisoo Park, Ph.D. student
Email: jpark711@gatech.edu

Contract with
Georgia Department of Transportation

In cooperation with
U.S. Department of Transportation
Federal Highway Administration

March 2019

The contents of this report reflect the views of the authors who are responsible for the facts and the accuracy of the data presented herein. The contents do not necessarily reflect the official views or policies of the Georgia Department of Transportation or Federal Highway Administration. This report does not constitute a standard, specification, or regulation.

TABLE OF CONTENTS

TABLE OF CONTENTS.....	iv
LIST OF TABLES.....	v
LIST OF FIGURES	vi
EXECUTIVE SUMMARY	viii
ACKNOWLEDGMENTS	xii
1. Introduction.....	1
2. Literature Review.....	3
2.1 Mass concrete specifications.....	3
2.2 Delayed ettringite formations (DEF).....	5
2.3 Thermal control methods	6
3. Objectives	7
4. Mid-Scale Heat of Hydration and Cooling Experiments (Task 1)	8
4.1 Compressive strength of proposed mix designs for mass concrete.....	8
4.2 Semi-adiabatic cylinder tests.....	11
4.3 Mid-scale heat of hydration and cooling system tests	14
4.3.1 Mid-scale test without a cooling system.....	14
4.3.2 Mid-scale test with a cooling system.....	16
5. Analytical Modeling of Cooling Experiments (Task 2)	19
5.1 Methodology	19
5.2 Analytical modeling of the mid-scale test without a cooling system.....	20
5.3 Analytical modeling of the mid-scale test with a cooling system.....	23
6. Development of Thermal Management Plan (Task 3).....	30
6.1 Decision-making framework.....	30
6.2 AHP analysis.....	31
6.2.1 AHP for passive cooling strategies (scenario 1).....	33
7. Conclusion	36
REFERENCES	39
Appendix A.....	41

LIST OF TABLES

Table 1. Mass concrete definitions in the United States	4
Table 2. Proposed mix designs for mass concrete	9
Table 3. The pairwise comparison matrix (3×3) for the criteria.....	32
Table 4. The normalized matrix (3×3) and the weight vector	33
Table 5. Cost information of the mix designs proposed in this study.....	33
Table 6. AHP results for passive strategies	34

LIST OF FIGURES

Figure 1. Mass concrete designations in the United States.....	3
Figure 2. Mass concrete specifications in the United States.....	4
Figure 3. A slump test for the baseline concrete.....	10
Figure 4. A scene of the compressive strength test.....	10
Figure 5. The results of the compressive strength tests	11
Figure 6. The insulated (left) and uninsulated (right) cylinders	12
Figure 7. The temperature increase in insulated cylinders	12
Figure 8. The temperature increase in uninsulated cylinders	13
Figure 9. The concrete form for the mid-scale specimen	14
Figure 10. The locations of the sensors	15
Figure 11. The results of the mid-scale specimen test (without cooling).....	16
Figure 12. Plan of the mid-scale test with the cooling system.....	17
Figure 13. The inside frame (left) and the cooling pipes (right).....	18
Figure 14. The results of the mid-scale specimen test (with cooling)	18
Figure 15. Heat generation history from Python code used in ABAQUS	20
Figure 16. 3D simulation results for the mid-scale test without a cooling system	21
Figure 17. Experimental vs. modeled temperature history in the core of the specimen (sensor location T4)	22
Figure 18. Experimental vs. modeled temperature history near the surface.....	23
Figure 19. 1D simulation of actively cooled concrete, various pipe materials, time evolution; location is 0.39 m above the bottom of the concrete, midway between cooling pipes (cooled steel = cooled copper).....	24
Figure 20. 1D simulation of actively cooled concrete, various pipe materials, spatial distribution (cooled steel = cooled copper).....	25
Figure 21. 1D simulation of actively cooled concrete, PEX tubing	26
Figure 22. Midscale experiment with active cooling vs. 1D FTCS Python simulation of actively cooled concrete using PEX tubing; the simulation data have been shifted by 1.2 hours to account for concrete transport.....	27
Figure 23. Adiabatic temperature rise at placement temperature of 20 °C (68 °F)	28
Figure 24. Adiabatic temperature rise at placement temperature of 30 °C (86 °F)	28
Figure 25. Adiabatic time rate of energy generation (Egen) at placement temperature of 20 °C (68 °F)	29
Figure 26. Adiabatic time rate of energy generation (Egen) at placement temperature of 30 °C (86 °F)	29
Figure 27. Decision-making process for mass concrete cooling	30

Figure 28. Framework for the AHP 31

EXECUTIVE SUMMARY

The Georgia Department of Transportation (GDOT) considers mass concrete as “any large volume of cast-in-place concrete with dimensions large enough to require that measures be taken to cope with the generation of heat and attendant volume change to minimize cracking.” The current GDOT specification requires contractors to develop and implement thermal management techniques (e.g., active cooling during curing, precooling prior to placement, etc.) to mitigate risks arising from high temperatures and thermal gradients in mass concrete. The bespoke nature of these measures often leads to a risk of the added expense of developing and enacting cooling measures. Standardized, validated cooling systems are seen as a way to mitigate this cost risk as the engineering expenses are spread over many projects. To address these issues on mass concrete, the objectives of this research are 1) to characterize the heat generation in mass concrete placements typically encountered by GDOT; 2) to create an analytical method for determining the cooling requirements for concrete; and 3) to develop a comprehensive guideline for transportation infrastructure applications. To achieve the objectives, the research team conducted four main tasks as follows.

- **Task 1. Mid-Scale Heat of Hydration and Cooling Experiments at Georgia Tech:** The research team developed new mix designs and assessed their performance for mass concrete by characterizing their compressive strength and heat of hydration characteristics. This included both small-scale, semi-adiabatic specimens and mid-scale specimen tests, one with integral cooling.

- **Task 2. Analytical Modeling of Cooling Experiments:** The research team created analytical thermal models, including both simple heat of hydration models and finite element models depicting heat generation and distribution of temperature in large placements of mass concrete and including the integration of cooling into mass concrete.
- **Task 3. Development of Thermal Management Plan:** The research team developed thermal management plans for mass concrete based on the results from Tasks 1 and 2. For this purpose, the analytic hierarchy process (AHP) analysis was conducted to identify the best practice on the mass concrete thermal control considering cost, performance, and feasibility. For the AHP analysis, the research team surveyed contractors throughout the country as well as GDOT engineers.
- **Task 4. Report and Workshop:** The research team hosted a progress meeting and workshop with GDOT engineers to demonstrate the research outcome.

Through the literature review, the research team found that two major concerns exist with mass concrete. The first is that large thermal gradients during the heat generation phase and subsequent cooling phase lead to a restraint of thermal movement and subsequent tension cracking in locations where the tensile stress in the concrete exceeds the tensile strength. The second is that high temperatures exceeding around 180°F will lead to delayed ettringite formation (DEF) in the concrete. At this time, the clear solution to both of these problems is to use Class F fly ash (FA) in all mass concrete. Class F fly ash is pozzolanic, tending to slow the set of chemical reactions associated with concrete curing; thus, it lowers both the heat of hydration release and the rate of strength increase in the concrete. In

addition, concrete made with fly ash tends to have a higher temperature threshold for DEF. For this reason, Florida DOT suggests a minimum fly ash content of 25% for all mass concrete, and it is proposed for GDOT to provide the same specification.

To support this, the research team tested a concrete mix with 25% Class F fly ash and a second mix with 45% Class F fly ash. The 25% mix demonstrates a modest reduction in the peak heat of hydration with good early strength gain. The 45% mix demonstrates a significant reduction in the peak heat of hydration, but with a significant delay in strength gain. The project team recommends that GDOT consider the 45% mix when it can be shown that the structural elements (e.g., foundations, pile caps, and piers) will not be subject to early loading. In addition, the team recommends that GDOT consider specifying 56-day strength requirements for these elements, instead of the 28-day strength requirements. Additionally, the project team recommends that GDOT assess the current special provisions for inadvertent requirements that exacerbate mass concrete problems. This modification is likely in place to ensure a uniform, flowable concrete mix in a situation where consolidation of the concrete is of concern. But workable, high-flowing mixes can be developed using other materials such as limestone, which provide workability without additional heat in the mix.

Through Task 2 (Analytical Modeling of Cooling Experiments), the research team found that the one-dimensional (1D) forward-time, centered-space (FTCS) model can closely predict peak temperatures and that three-dimensional (3D) finite-element analysis (FEA) models slightly over-predict peak temperatures. All models under-predict the rate of

temperature change within concrete when the concrete is not actively cooled. The 1D FTCS model over-predicts the rate of temperature decrease under active cooling. It is suspected that the equations generating the parameters of the theoretical energy generation (Egen) equation may be out of date with current cement mixes; however, other impacts, such as inaccurate concrete properties, like specific heat or density, have not been ruled out. Despite discrepancies with experiments, the 1D FTCS and 3D FEA models nevertheless facilitate the design of effective active cooling systems. The 1D model enables quick estimates of the impact of pipe size, material, and spacing; water temperatures; and water flow rates. However, it does not capture the multidimensional effects that the FEA model does. In practice, the 1D model was used to generate an initial cooling system design that was refined using the FEA model.

With the outcomes from Tasks 1 and 2, the research team conducted AHP analysis to identify the best practice for mass concrete. From a result of an online survey with contractors and GDOT engineers, the importance weights of the criteria were determined as follows: 1) cost: 0.322; 2) performance: 0.406; and 3) feasibility: 0.273. With the importance weights, the research team completed AHP analysis on a passive strategy. According to the results, fly ash (FA) + blast furnace slag (BFS) concrete was the best alternative for mass concrete structures, and coarse cement concrete was second. These results were based on the cost information collected by a concrete supplier in Georgia and the experiment results in this study. The price and availability of concrete mixtures depend on the region, and therefore, results may vary from region to region.

ACKNOWLEDGMENTS

The research reported herein was sponsored by the Georgia Department of Transportation through Research Project Number 16-25. The authors acknowledge and appreciate the help from Mr. Andy Carroll, Project Manager of Scott Bridge Company, Inc. The authors would also like to thank Mr. John Hancock, State Construction Engineer, Mrs. Supriya Kamatkar, Research Program Manager, Mr. Marc Mastronardi, Director of Construction, and Mr. Beau Quarles, Assistant State Construction Engineer at the Georgia Department of Transportation who have helped us throughout the progress of this research project. In addition, the authors heartily thank the GDOT engineers participated in our workshop.

1. Introduction

The Georgia Department of Transportation (GDOT) defines mass concrete as “any large volume of cast-in-place concrete with dimensions large enough to require that measures be taken to cope with the generation of heat and attendant volume change to minimize cracking” and regulates that “any concrete element with the least dimension greater than 5 ft. (or greater than 6 ft. diameter for a drilled shaft) shall be designated as mass concrete.” GDOT permits contractors to utilize approved methods for mass concrete cooling as long as a temperature differential of 35°F or less is maintained between the interior and exterior portions of the designated mass elements, and the maximum internal temperature of mass concrete does not exceed 158°F (Georgia Department of Transportation, 2013).

The current GDOT specification requires contractors to develop and implement thermal management techniques (e.g., active cooling during curing, precooling prior to placement, etc.) to mitigate risks arising from high temperatures and thermal gradients in mass concrete. The bespoke nature of these measures often leads to a risk of the added expense of developing and enacting cooling measures. Standardized, validated cooling systems are seen as a way to mitigate this cost risk as the engineering expenses are spread over many projects. To mitigate the risks, researchers, as well as members of other state construction and structures divisions, have been evaluating and implementing specifications regarding the methodology of mass concrete cooling.

For example, the California Department of Transportation (CalTrans) Division of Research and Innovation investigated the effects of the heat of hydration of mass concrete for cast-

in-place piles (Al-Manaseer & Elias, 2008). Through a series of studies on mass concrete, several DOTs have developed their own mass concrete specifications and specific methods of cooling mass concrete structures to ensure the quality of the structure (FDOT, 2015; Georgia Department of Transportation, 2013). In most cases, however, they provided only passive methods that replace some proportion of cementitious material with other admixtures, such as fly ash and blast furnace slag (BFS). Moreover, most specifications require a consistent mass concrete design for concrete elements over a certain size, despite the fact that the heat of hydration of concrete varies greatly depending on the size of the elements and the surrounding environment. To address these problems, this study proposes a decision-making framework to apply a proper mass concrete cooling method according to the size of the mass concrete structures and the surrounding environment. In addition, this study suggests optimal alternatives for passive and active cooling methods based on the results of the analytic hierarchy process (AHP).

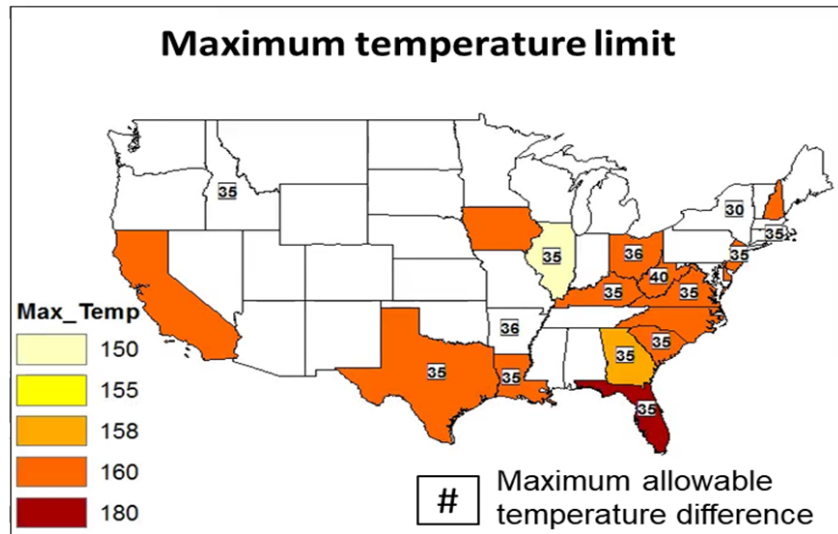


Figure 2. Mass concrete specifications in the United States

As shown in Figure 2, only Florida lists a maximum temperature of 180°F. This is because the Florida DOT has not approved a concrete mixture to be used for mass concrete applications without slag or fly ash, based on several studies indicating that the delayed ettringite formation (DEF) is mitigated in fly ash and slag concrete (Chini, Muszynski, Acquaye, & Tarkhan, 2003). Table 1 shows the variation in definitions in the United States.

Table 1. Mass concrete definitions in the United States

State DOT	Definition
California	<ul style="list-style-type: none"> • CIP pile with a diameter greater than 8 ft. (2.4 m) and temperature monitoring required for diameter greater than 14 ft. (4.3 m) • All other elements with least dimension greater than 7 ft. (2.1 m)
Florida	<ul style="list-style-type: none"> • Concrete with the least dimension of 3 ft. (0.9 m) where the volume to surface area of the concrete exceeds 1 ft. (0.3 m) • Drilled shafts with a diameter greater than 6 ft. (1.8 m)
Georgia	<ul style="list-style-type: none"> • Any element with least dimension greater than 5 ft. (1.5 m) • Any drilled shaft with least dimension greater than 6 ft. (1.8 m)

Table 1. Mass concrete definitions in the United States (Continued)

State DOT	Definition
Illinois	<ul style="list-style-type: none">• Least dimension of 5 ft. (1.5 m) for drilled shafts, foundations, footings, substructures, or superstructures
Kentucky	<ul style="list-style-type: none">• Any structural element, excluding drilled shafts, with least dimension greater than 6 ft. (1.8 m)
Louisiana	<ul style="list-style-type: none">• Any concrete placement with least dimension greater than 4 ft. (1.2 m)
Texas	<ul style="list-style-type: none">• Any concrete placement, excluding drilled shafts, with least dimension greater than 5 ft. (1.5 m)

2.2 Delayed ettringite formations (DEF)

The temperature of hydraulic cement rises as the mixing of the material causes chemical reactions, which is defined as the heat of hydration. Most factors influencing the hydration process also affect the rate of heat development and should be assessed in a mechanistic modeling procedure (Al-Manaseer & Elias, 2008). Main factors impacting the hydration heat in mass concrete structures include amount and type of cement, water content, conditions of the surrounding environment, thermal properties, and structural geometric properties. The temperature of the inner structure will peak a few days after the concrete is placed; this is followed by cooling to a stable temperature (Mindeguia, Pimienta, Noumowé, & Kanema, 2010). During the rising temperature phase, a DEF can occur if the internal temperature exceeds a critical value. The DEF is an internal form of concrete deterioration. Volume changes impact the temperature change, which influences the amount of thermal expansion for the concrete. For example, as concrete is placed in formwork, the volume change is restrained during the cooling process, which builds a tensile strain sufficient to cause internal cracks and deterioration.

2.3 Thermal control methods

Two variables are required to minimize cracking in mass concrete structures. These variables are the temperature differential and the maximum temperature of the concrete material. The following four methods are typically implemented as thermal control methods (Riding, Poole, Schindler, Juenger, & Folliard, 2006):

- Lowering concrete mixture heat by maximizing cement replacement and minimizing cementitious concrete – passive control
- Pre-cooling fresh concrete by shading or sprinkling aggregates, chilling batch water, replacing batch water with ice or adopting liquid nitrogen – active control
- Applying thinner placements to quicken the cooling process – active control
- Implementing post-cooling systems – active control

Thermal control methods can be described as passive or active controls. Passive controls, which are implemented prior to concrete placement, control the concrete ingredients, the placement temperature and the mass of the structure. Active controls, which occur during the hydration period, use insulating blankets to limit the temperature differentials. Active controls also include installation of cooling pipes to accelerate internal heat exchange and control the maximum temperature (Gajda & Vangeem, 2002).

3. Objectives

Currently, a common standard for cooling methods for mass concrete does not exist. Minimal recommendations for thermal management during mass concrete cooling are available. To provide objective data for decision making about mass concrete cooling, this research aims to:

1. characterize the heat generation in mass concrete placements typically encountered by GDOT in its construction projects,
2. create an analytical method for determining the cooling requirements for concrete,
3. and develop a comprehensive guideline for applying proper cooling methods to mass concrete structures.

4. Mid-Scale Heat of Hydration and Cooling Experiments (Task 1)

To obtain objective data on the methods of hydration heat control of mass concrete, the research team conducted several tests as follows:

1. compressive strength of proposed mix designs for mass concrete – ASTM C 39
2. semi-adiabatic cylinder tests – ASTM C 1768
3. mid-scale (4x4x6 ft.) heat of hydration and cooling system tests

The results of the compressive strength and hydration heat tests were used as references for creating the best practice guidelines.

4.1 Compressive strength of proposed mix designs for mass concrete

In this study, the research team proposes five mix designs for mass concrete based on the results of the literature reviews. Table 2 shows the five mass concrete mix designs and a baseline concrete. The target slump was from 6 to 8 in. Figure 3 depicts a slump test conducted with baseline concrete. In this experiment, GDOT class AA concrete was used as a baseline concrete (Georgia Department of Transportation, 2006). In addition, type-F fly ash and 40 μm limestone were used in this study. A total of 24 compression tests for the six mix designs were conducted at the end of the 7th, 14th, 28th, and 56th days of curing, and the tests followed ASTM C 39. Three concrete cylinders were used for each compression test. The results were calculated as the average of the compressive strengths of the three cylinders. Figures 5 shows the results of the compressive strength tests.

Table 2. Proposed mix designs for mass concrete

		Baseline	45% FA	25% FA	FA + BFS	Coarse cement	Limestone
Cementitious material (lb./cu. yd.)	Cement	696.6	379.8	521.3	410.4	525.6	696.6
	Slag	-	-	-	165.6	-	-
	FA (type F)	-	315	173.8	124.2	-	-
	40 μm limestone	-	-	-	-	174.6	-
	Total binder	696.6	364.8	695.0	700.2	700.2	696.6
	Water	340.2	342	327.3	342	309.6	309.6
	W/C	0.488	0.492	0.471	0.488	0.442	0.444
Aggregate (lb./cu. yd.)	#67	1684.8	1684.8	1701.0	1684.8	1701.0	1701.0
	Natural sand	1254.6	1213.2	1226.0	1180.8	1267.2	1267.2
	Coarse/fine ratio	1.34	1.39	1.39	1.43	1.34	-
	PCWR	13.932	13.896	20.850	14.004	14.004	13.932

*FA: fly ash, BFS: blast furnace slag, PCWR: polycarboxylate superplasticizer water reducer, W/C: water-cementitious material ratio



Figure 3. A slump test for the baseline concrete



Figure 4. A scene of the compressive strength test

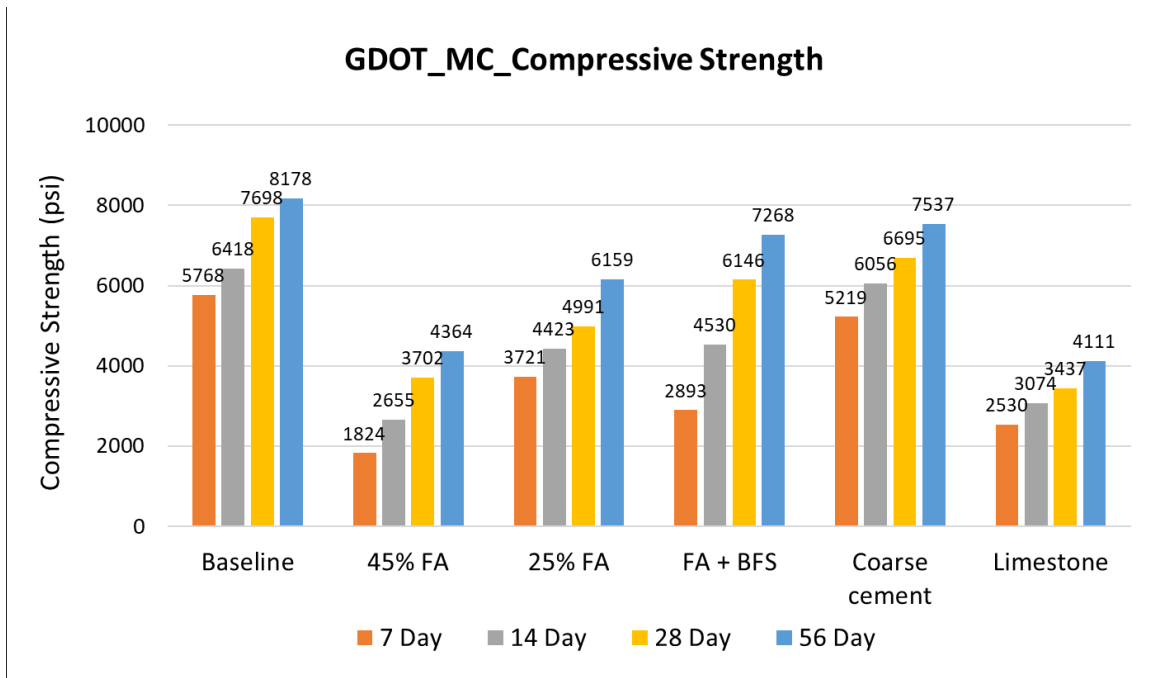


Figure 5. The results of the compressive strength tests

The results demonstrated that the higher the content of fly ash, the lower the compressive strength. The limestone concrete showed similar compressive strength to the fly ash concrete, and the coarse cement concrete showed the highest compressive strength among the proposed mix designs.

4.2 Semi-adiabatic cylinder tests

To examine the heat of hydration for each concrete mixture, the research team conducted semi-adiabatic cylinder tests with the six mix designs used in the compressive strength tests. For this purpose, the research team prepared insulated/uninsulated 6×12-in. cylinders with low-modulus strain/temperature sensors, as seen in Figure 6. The test followed ASTM C1768 (ASTM, 2017).



Figure 6. The insulated (left) and uninsulated (right) cylinders

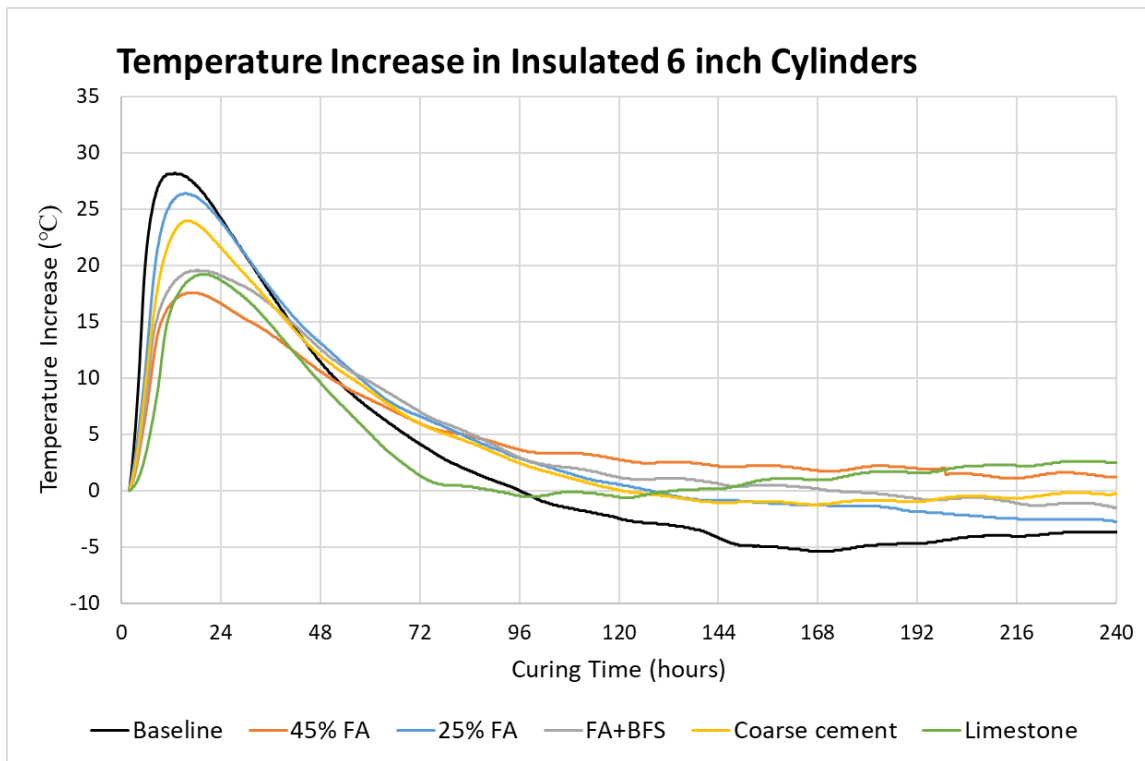


Figure 7. The temperature increase in insulated cylinders

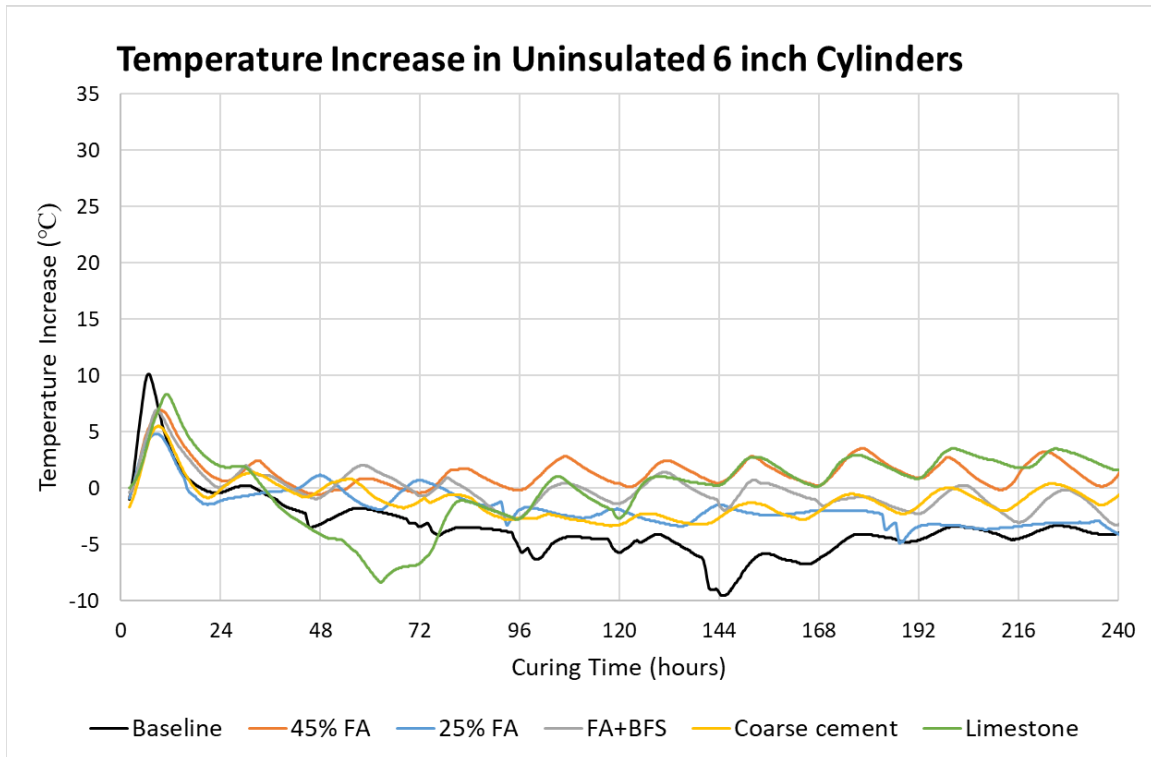


Figure 8. The temperature increase in uninsulated cylinders

Figures 7 and 8 depict the temperature increase in insulated cylinders and uninsulated cylinders respectively. With the results of the compression tests and the semi-adiabatic cylinder tests, the research team found that the 25% fly ash mix demonstrated a modest reduction in the peak heat of hydration with reasonable early strength gain. The 45% mix demonstrated a significant reduction in the peak heat of hydration, but with a significant delay in strength gain. Therefore, the research team recommends that GDOT consider the 45% mix when it can be shown that the structural elements (e.g., foundations, pile caps, piers) will not be subject to early loading. Since the tests were conducted on different dates, the ambient temperatures were also different. Therefore, to acquire more reliable data, the tests should be performed again on the same date.

4.3 Mid-scale heat of hydration and cooling system tests

The research team built a mid-scale (4×4×6 ft.) specimen to characterize the internal heat generation of different mix designs and associated stresses. The specimen contained approximately 3.6 cubic yards of concrete weighing around 15,000 pounds. The specimen was instrumented with the temperature sensors and concrete strain gauges to directly measure the temperature increases caused by hydration heat and compressive stresses associated with the restraint of expansion and of shrinkage caused by differential temperature changes and by differential shrinkage. Figure 9 is an image of the assembled concrete form for the mid-scale specimen.



Figure 9. The concrete form for the mid-scale specimen

4.3.1 Mid-scale test without a cooling system

The first experiment was conducted with the baseline concrete without a cooling system inside. The specimen is configured to promote one-dimensional heat flow (one cool surface

at the top) and also a zone near the bottom that exceeds the temperature for delayed ettringite formation (DEF). In order to collect the data, several sensors were installed. Thirteen sensors were used for the specimen; the detailed information and the installed locations are shown in Figure 10.

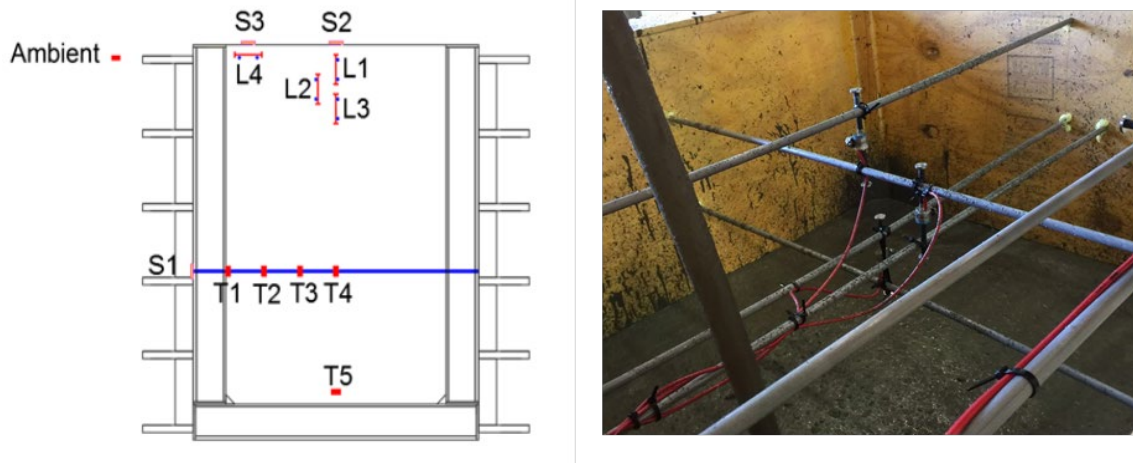


Figure 10. The locations of the sensors

The four low-modulus strain/temperature sensors were positioned to capture the tensile stresses caused by the differential temperature at the heat flow boundary. Additional embedded temperature sensors (thermistors) were located near the boundaries of the formwork to assess the efficacy of our insulation scheme and to help calibrate the finite element models. Surface temperatures were measured on the uninsulated surface and on the surface of the formwork. The data collecting interval was 5 minutes for the first 14 days and every 15 minutes for the remaining 16+ days required for the specimen to cool.

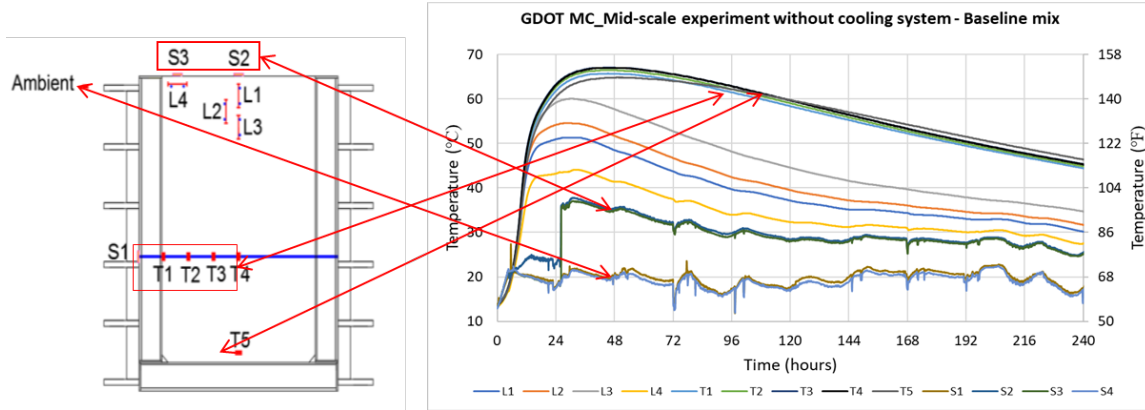


Figure 11. The results of the mid-scale specimen test (without cooling)

The temperature data collected by the sensors in the mid-scale specimen are shown in Figure 11. The maximum temperature was 152.78°F (67.1°C) for T3 after casting the concrete 46 hours. The maximum temperature difference between the surface (S2) and the core (T3) of the concrete specimen was 48.5°F (27.1°C).

4.3.2 Mid-scale test with a cooling system

The research team also conducted a second mid-scale test with the cooling system. In this test, 25% fly ash concrete was used. The research team rebuilt the formwork and fabricated inside frames for installing sensors and cooling systems as shown in Figure 12. A total of six thermal sensors and nine strain-thermal sensors were installed to the frame in the formwork, and three thermal sensors were installed on the top surface. The schematic of the planned experiment is shown in Figure 13. The experiment featured four cooling loops. All four of the loops were made of PEX, both for high flexibility and to remove the need for excess connections. The flow rate was measured at 15 gallons per minute (GPM), meeting the cooling requirements.

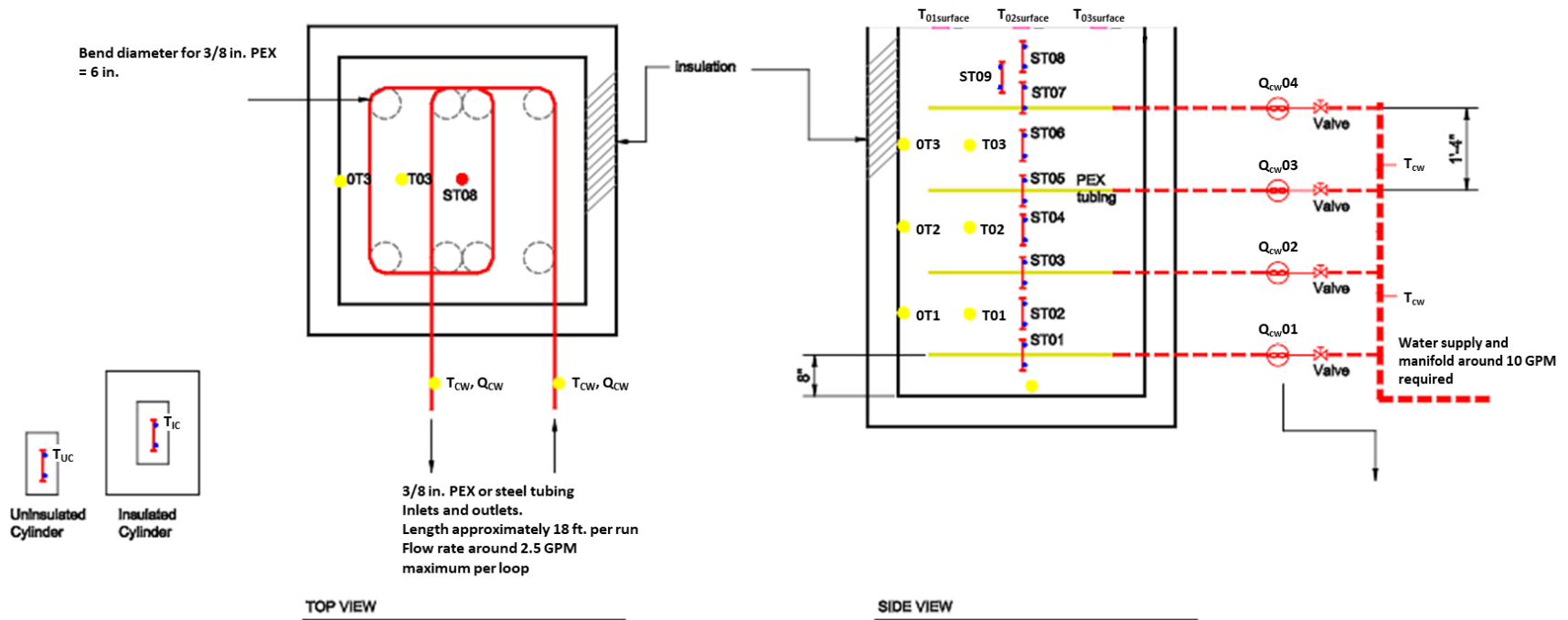


Figure 12. Plan of the mid-scale test with the cooling system



Figure 13. The inside frame (left) and the cooling pipes (right)

The temperature data collected by the sensors in the mid-scale specimen are shown in Figure 14. The cooling started 14 hours after concrete casting and lasted for eight hours. The maximum temperature was 139.28°F (59.6°C) for TS 4 (temperature of ST04) 17 hours after concrete casting. After cooling started, the temperature decreased to 126.1°F (52.3°C). The results of comparative analysis between experiment and simulation are explained in Section 5.

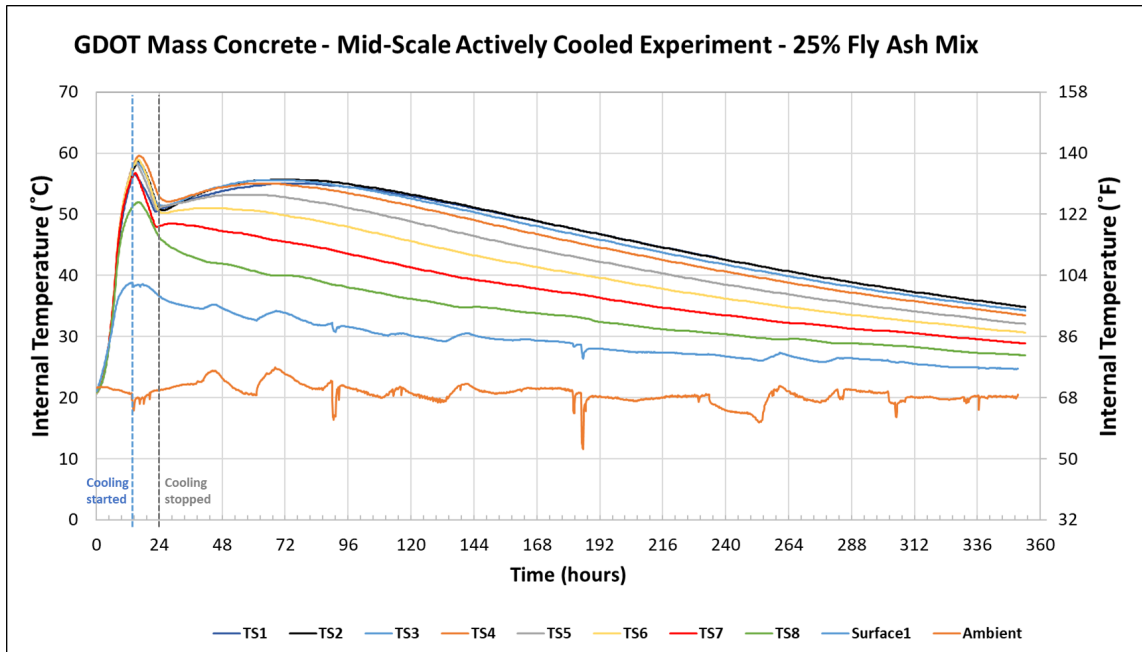


Figure 14. The results of the mid-scale specimen test (with cooling)

5. Analytical Modeling of Cooling Experiments (Task 2)

The research team created analytical thermal models, including finite element models depicting the distribution of temperature in large placements of unreinforced mass concrete. The main goal of these analytical investigations was to provide guidance for the development of the thermal management plan in Task 3. In addition, the mid-scale test data was used to calibrate and verify the analytical models. The research team intended to identify relations between key variables in order to support decisions regarding thermal cooling system design and application, including characterizing the performance of heat removal systems configured using PEX, steel, and copper pipe, to enable cost-effectiveness to be addressed in the thermal management plan.

5.1 Methodology

To enable rapid modeling, a quasi-one-dimensional forward-time, centered-space (FTCS) finite difference model was initially implemented in a Microsoft Excel spreadsheet, but later written in a computer programming language, Python. This model solved the one-dimensional heat diffusion equation with a term describing the exothermic energy release due to cement hydration, and a correction term to account for heat transfer through the insulated formwork (Riding, Poole, Folliard, Juenger, & Schindler, 2012; Schindler & Folliard, 2005). In addition to computing temperatures and heat transfer within concrete under non-adiabatic conditions, the model also determined adiabatic quantities such as adiabatic temperature rise. This model also incorporated a simple scheme to model the impact of active cooling by water flowing through tubes; factors such as water temperatures and flow rates, and pipe materials and sizes, were included in the model as well.

5.2 Analytical modeling of the mid-scale test without a cooling system

Modeling of the mid-scale experiment has been conducted both in a one-dimensional model and in 3D finite elements using ABAQUS. One-dimensional modeling had previously been completed using a spreadsheet-based FTCS (forward time, centered-space) model; however, this version was difficult to maintain and enhance with new capabilities, such as modeling the thermal effects of formwork and incorporating a basic, simple model of active cooling systems. Thus, a Python code has been written to provide this more flexible, quick-turnaround modeling capability used to inform experimental design, aid in understanding test results, and support subsequent, more detailed analyses in ABAQUS. For example, the heat generation in concrete is more easily determined with this code, and this heat generation is used in the ABAQUS model as shown in Figure 15.

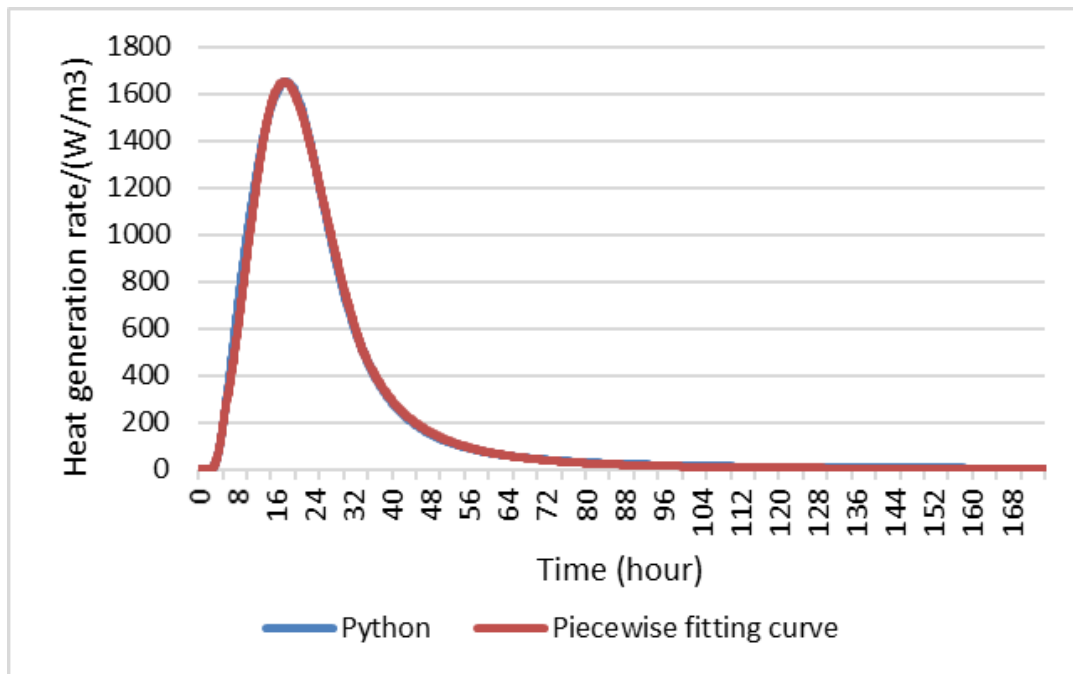


Figure 15. Heat generation history from Python code used in ABAQUS

Figure 16 shows the results of the 3D modeling and simulation using ABAQUS, and Figure 17 depicts experimentally measured temperature histories at sensor T4 (see Figure 10) along with temperatures simulated in ABAQUS and the one-dimensional Python model for the same location. Figure 17 shows the temperature profiles at the center of $z=0.66\text{m}$ of different simulation methods. In Figure 17, peak temperatures are well predicted, particularly for the Python simulation (153°F (67.1°C) experiment, 154°F (68°C) Python simulation), although the temperature history in the simulation lags compared to the experiment.

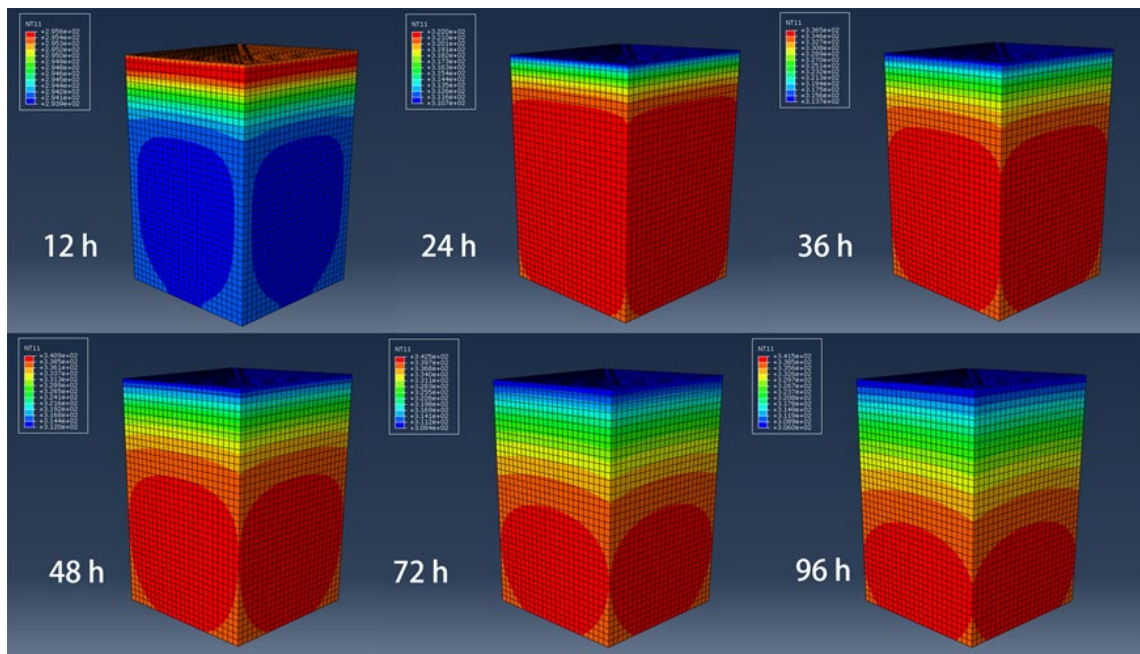


Figure 16. 3D simulation results for the mid-scale test without a cooling system

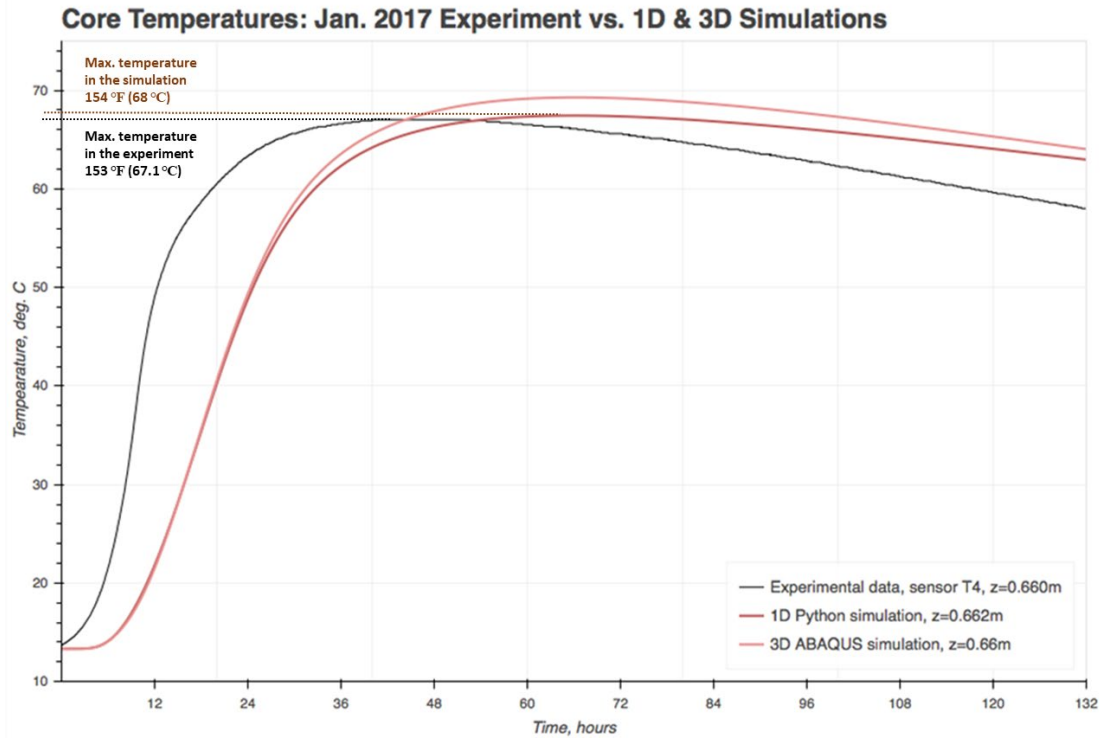


Figure 17. Experimental vs. modeled temperature history in the core of the specimen (sensor location T4)

Figure 18 shows the experimental surface and ambient temperatures along with similarly located simulated temperatures for both numerical models. Results show rough agreement in rate of cooling at the surface despite warmer simulated temperatures; this is perhaps due to 1) an under-specification of the boundary condition at the top surface in the simulations; and 2) in the case of the 1D simulations, the concrete is discretized in finite layers such that simulated temperatures are applied to all points within each layer; therefore the top layer's temperature is likely greater than that of the top surface of the concrete.

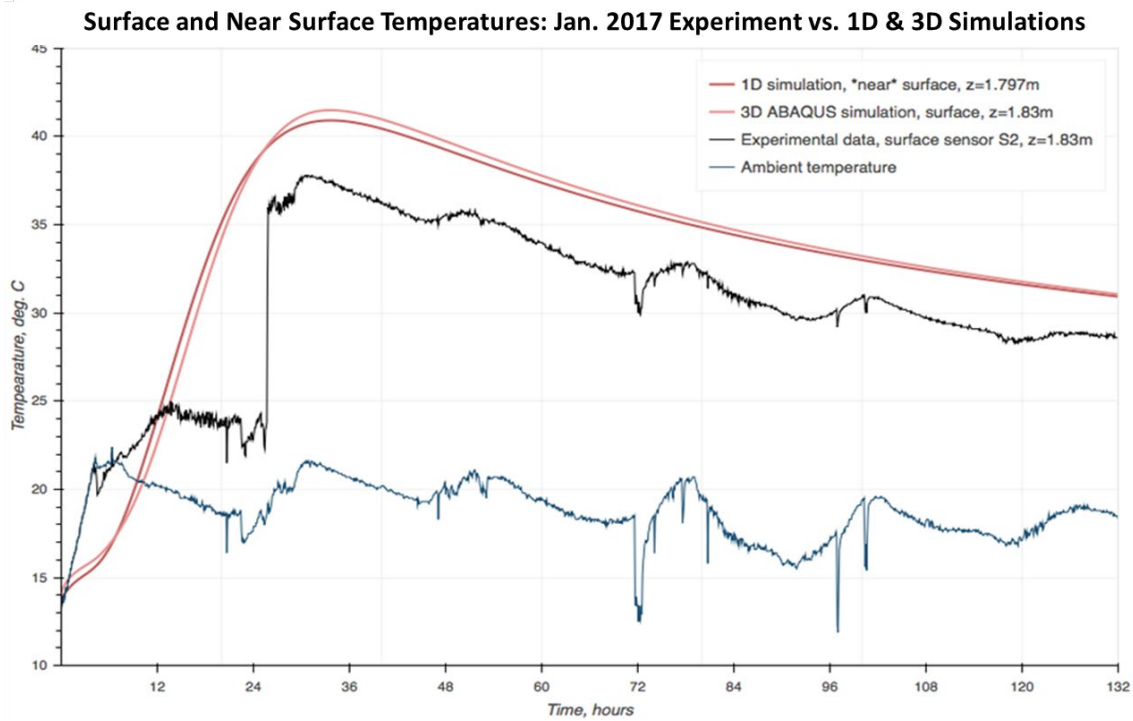


Figure 18. Experimental vs. modeled temperature history near the surface

5.3 Analytical modeling of the mid-scale test with a cooling system

The quasi-one-dimensional Python code supported the design of the mid-scale test with the cooling system. In addition to supporting decisions on pipe placement and diameter, the choice of material was taken in light of simulations. Figures 19 and 20 show the temperature evolution and spatial temperature distribution for the 25% fly ash mix under active cooling using 3/8-in. pipes made of PEX, steel, and copper; an uncooled simulation is provided for context. The temperature vs. time comparison (Figure 19) is for a location midway between cooling pipes, while the temperature vs. height above the bottom of the concrete plot (Figure 20) is for hour 23 of the simulation, roughly halfway to the conclusion of active cooling. The conditions are for the same as realized in the experiment: 1.7 GPM of 56°F water (simulations are run with identical mass flow rates of water, so the volume flow rates are slightly different for each material due to slight differences in actual pipe

dimensions). Cooling begins when any point in the concrete reaches 136°F (58°C) and ends when the hottest point in the concrete cools to 131°F (55°C).

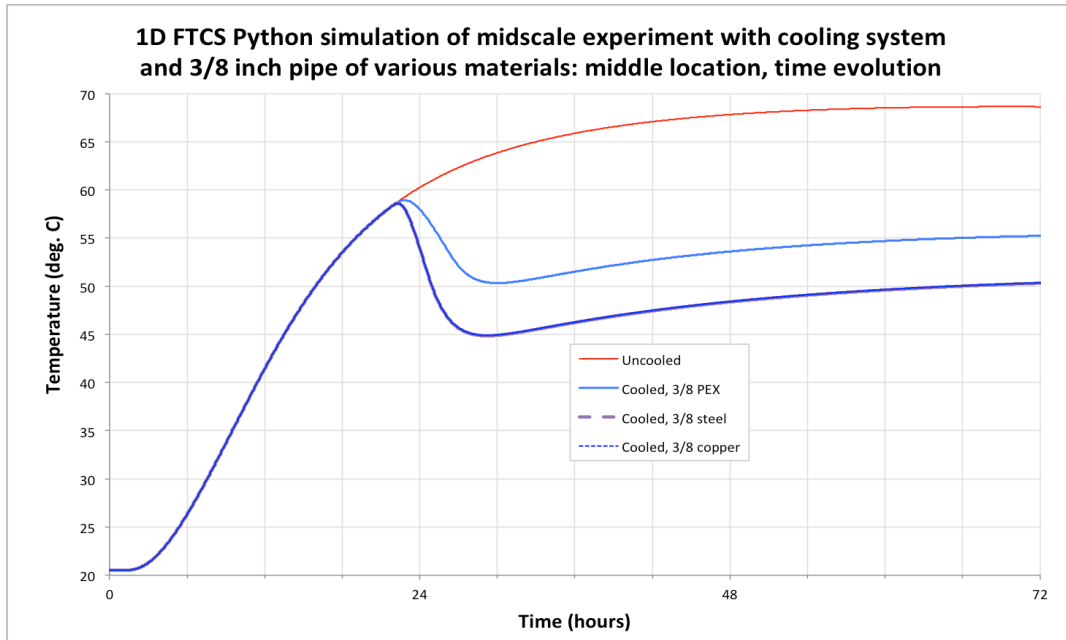


Figure 19. 1D simulation of actively cooled concrete, various pipe materials, time evolution; location is 0.39 m above the bottom of the concrete, midway between cooling pipes (cooled steel = cooled copper)

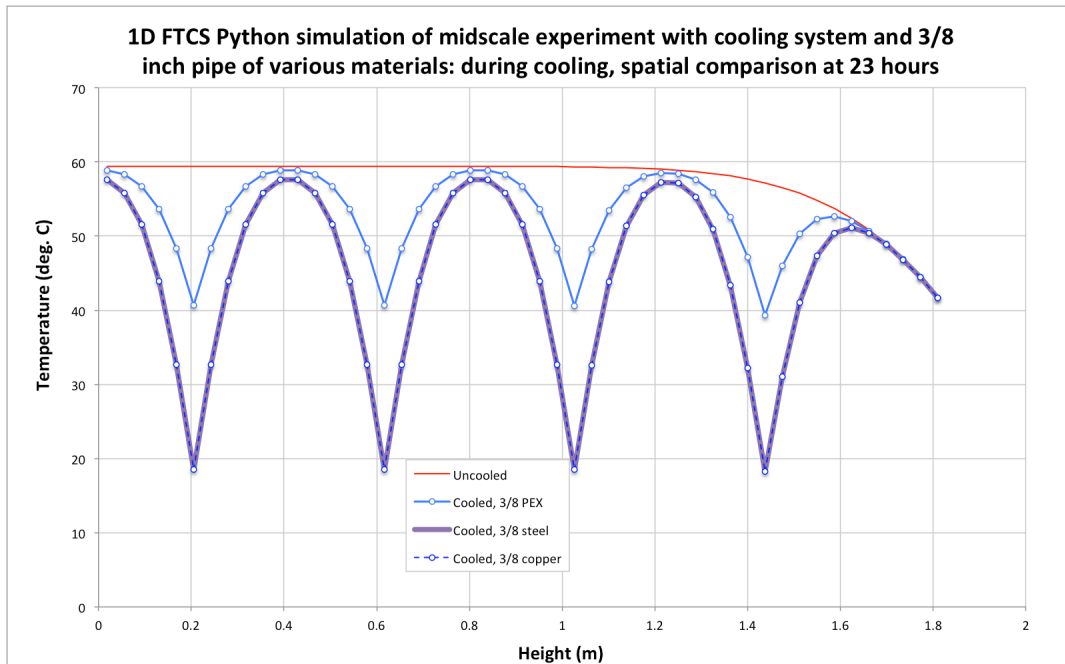


Figure 20. 1D simulation of actively cooled concrete, various pipe materials, spatial distribution (cooled steel = cooled copper)

Steel and copper tubing yield virtually identical results despite thermal conductivities that differ by a factor of 10. PEX, having a thermal conductivity 100 times smaller than steel, does have a lower cooling capability and requires just under two additional hours of active cooling in order for concrete to cool to 131°F (55°C); additionally, because the concrete in the vicinity of the pipes does not cool as much as with metal pipes, the concrete midway between actively cooled sections likewise does not cool as much as with metal pipes. However, for this mix, control scheme, pipe, and water temperature and flow rate, the concrete’s temperature never rises to a critical level after active cooling ceases.

Although the results above are for the same conditions (placement temperature, ambient temperature, etc.) as in the midscale experiment with active cooling, previous simulations led to similar conclusions, and so PEX tubing was chosen for the experiment on the basis

of cost and to demonstrate cooling with an inexpensive but thermally adequate material. Figure 21 shows simulated temperatures along a vertical profile of this experiment at times before, during, and after cooling with 1.7 GPM of 56°F water through 3/8-in. PEX tubes at the same locations as the physical experiment.

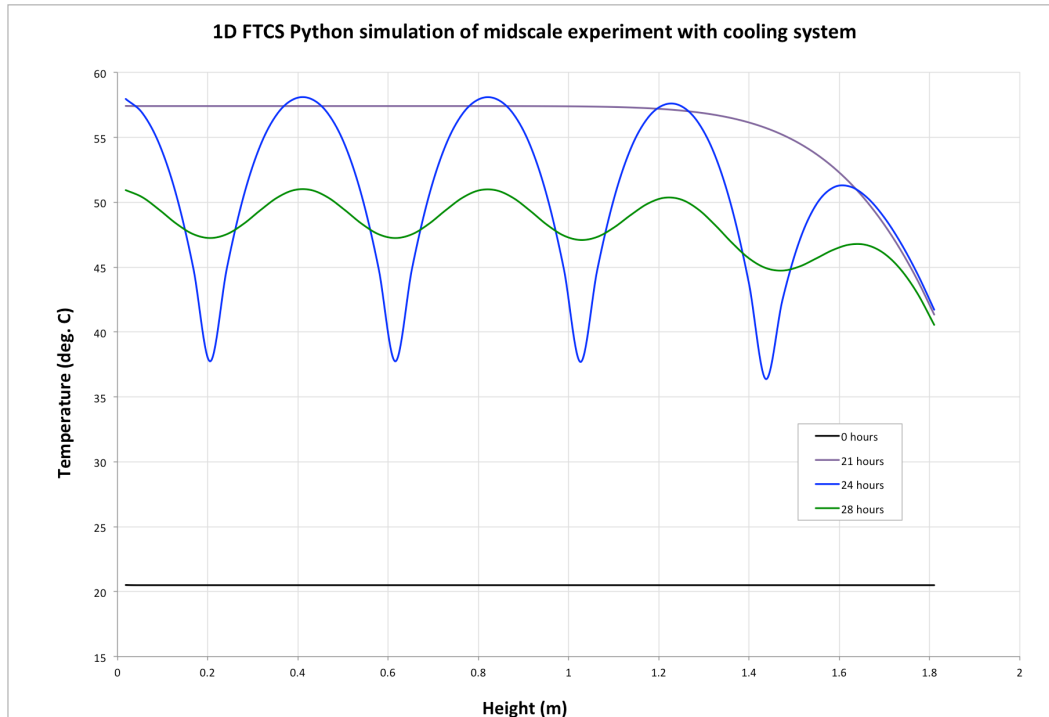


Figure 21. 1D simulation of actively cooled concrete, PEX tubing

As before, the cooling water begins flowing when the concrete reaches 136°F (58°C) – just after 21 hours in this simulation – and turns off once the concrete cools to below 131°F (55°C) 4 hours later. Compared to the physical experiment, the simulation under-predicted the rate of initial concrete heating, under-predicted the rate of passive cooling, and over-predicted the rate of active cooling, as shown in Figure 22. This under-prediction in the rate of heating and passive cooling was observed in both experiments (see Figure 21; note in this figure that the simulation data have not been time-shifted to account for concrete

transport, as they have for Figure 22). However, in both experiments, simulated peak temperatures are similar to those observed.

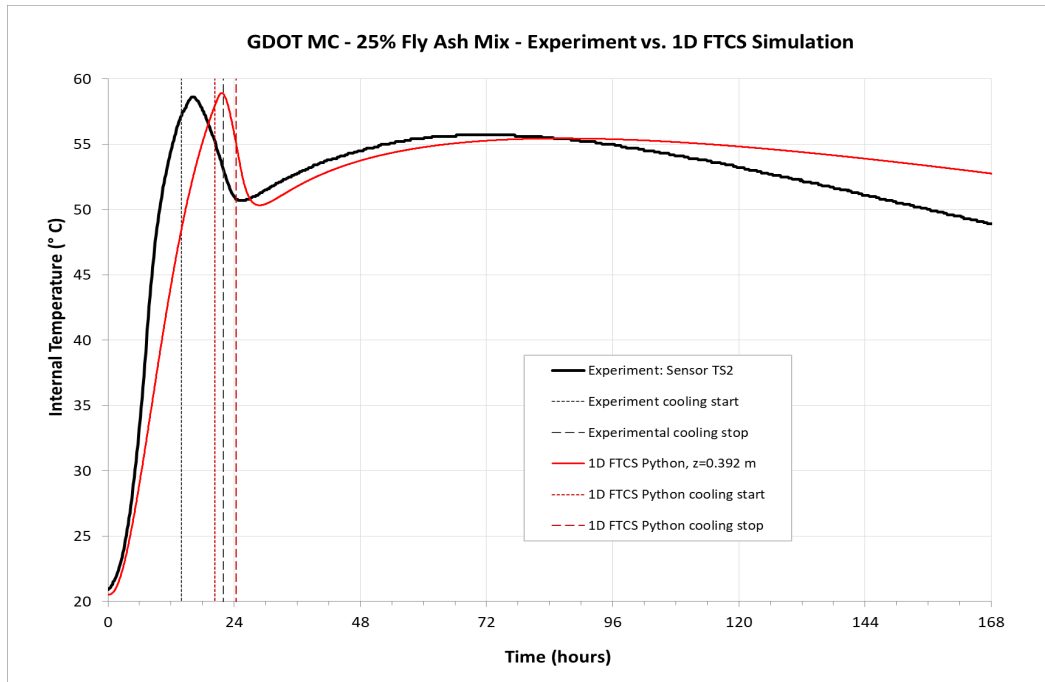


Figure 22. Midscale experiment with active cooling vs. 1D FTCS Python simulation of actively cooled concrete using PEX tubing; the simulation data have been shifted by 1.2 hours to account for concrete transport

The 1D Python code was also used, in a modified form, to compute the adiabatic behavior of six concrete mixes and two placement (initial) temperatures in order to examine a worst-case scenario and to explore the impact of lowering placement temperatures. Above a certain size, curing concrete exhibits a “core” region where temperatures are spatially uniform, and therefore, since there can be no conduction heat transfer, this core acts as if it were curing under adiabatic conditions with temperatures reaching their maximum possible values. Figure 23 and 24 depict adiabatic temperature rises, showing that a 1°F (or 1°C) increase in placement temperature results in a roughly 1°F (or 1°C) increase in final (maximum) temperature.

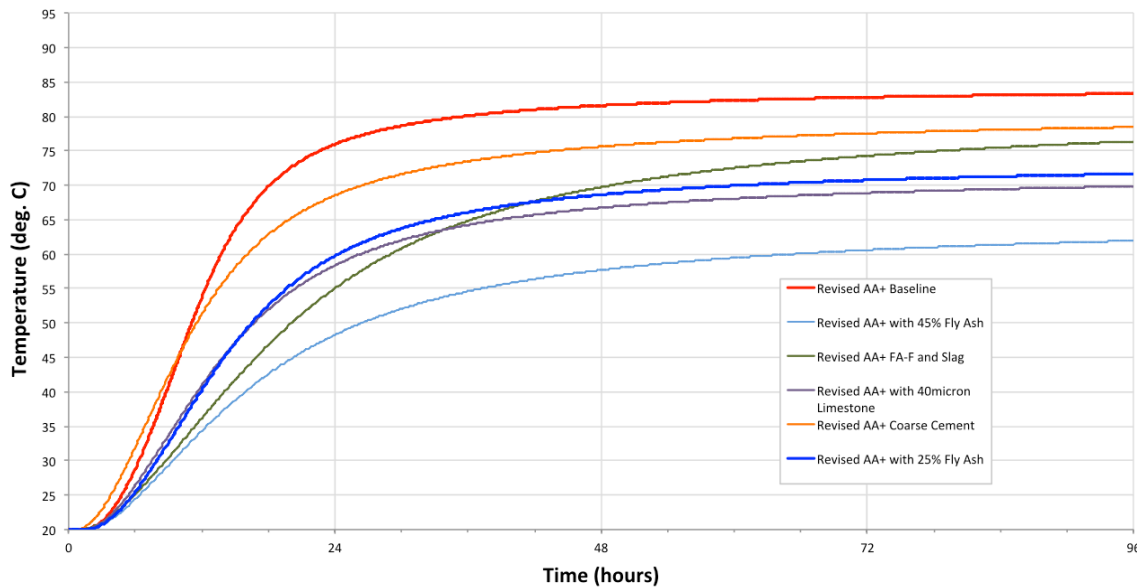


Figure 23. Adiabatic temperature rise at placement temperature of 20 °C (68 °F)

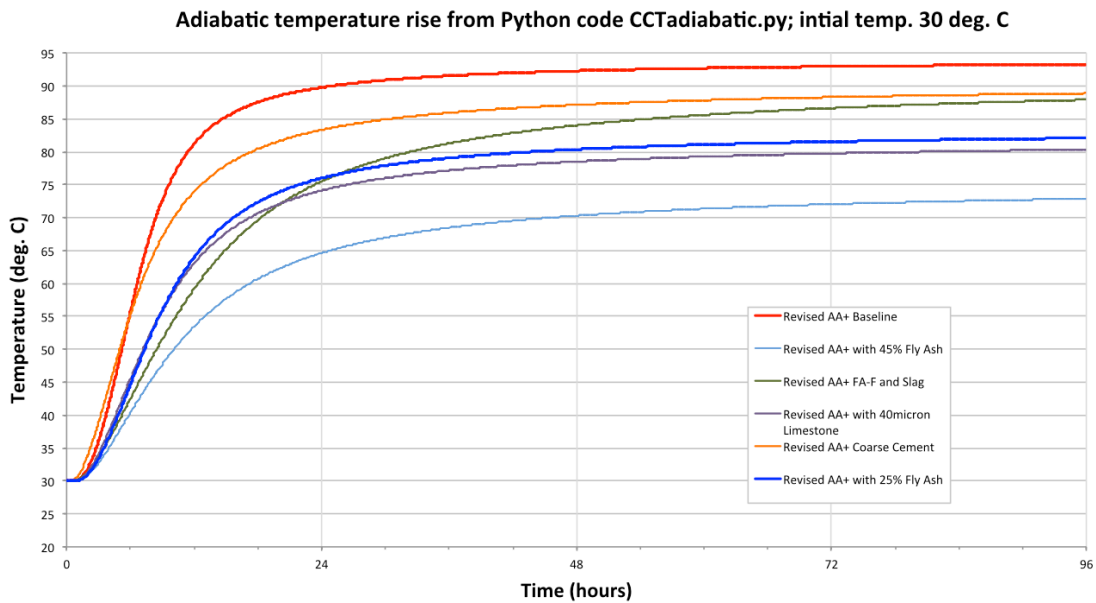


Figure 24. Adiabatic temperature rise at placement temperature of 30 °C (86 °F)

Increased placement temperatures also increase rates of heating dramatically, as shown in Figure 25 and 26; internally for this project, the volumetric exothermic release is referred to as “Egen” or (time rate of) energy generation.

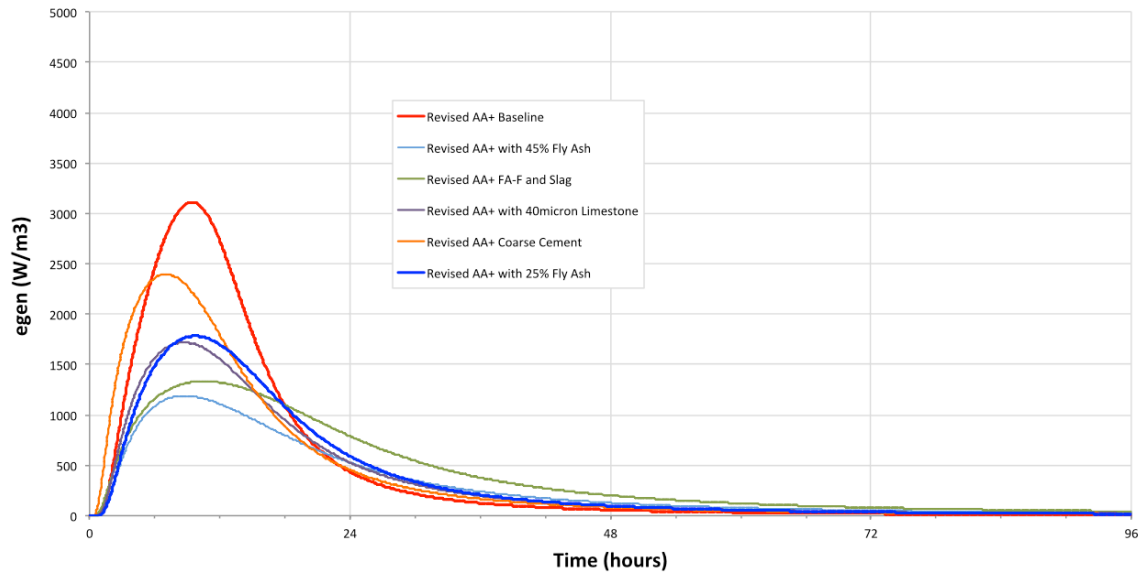


Figure 25. Adiabatic time rate of energy generation (Egen) at placement temperature of 20 °C (68 °F)

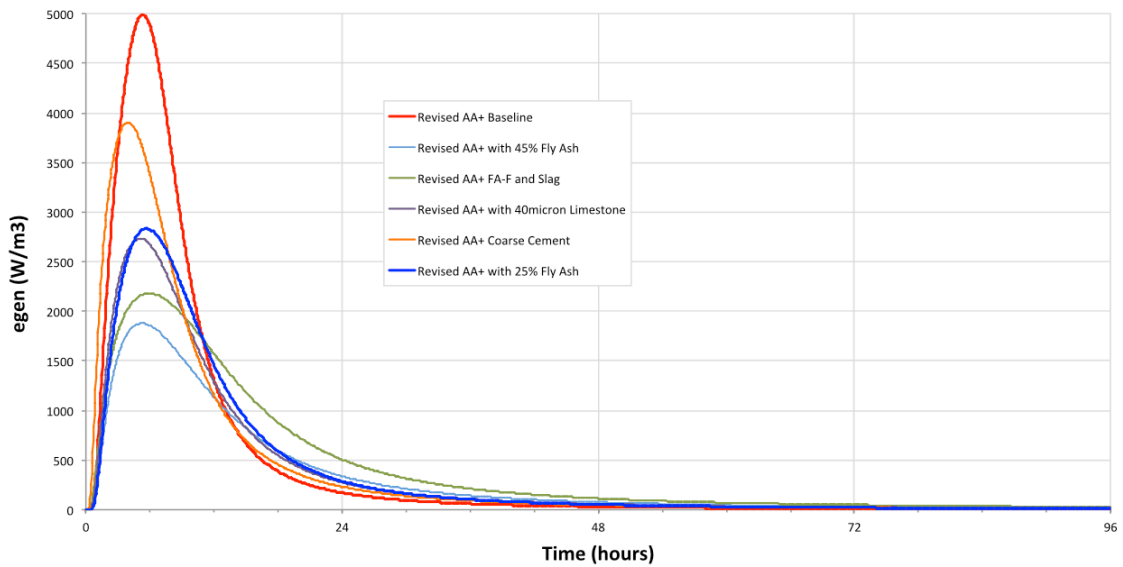


Figure 26. Adiabatic time rate of energy generation (Egen) at placement temperature of 30 °C (86 °F)

6. Development of Thermal Management Plan (Task 3)

Based on the results of Tasks 1 and 2, the research team developed thermal management plans, including a decision-making framework and analytic hierarchy process (AHP). The aim of the thermal management plan is to select an optimal alternative in various cooling methods considering performance, cost, and feasibility.

6.1 Decision-making framework

A framework for a decision making for thermal control plans for the mass concrete structure was developed, as shown in Figure 27. The proposed process begins with inputting specifications and determining whether the structure is defined as mass concrete in the specifications. After that, a proposed thermal modeling process developed in Task 2 is applied for determining whether a passive thermal control plan is enough to control the maximum temperature and temperature difference; if not, active thermal control plans should be selected. The definitions of passive strategies and active strategies are stated in the literature review section (section 2.3). After deciding on passive or active strategies, the framework specifies AHP analysis to select an optimal alternative. The details of the AHP analysis are demonstrated in the next section.

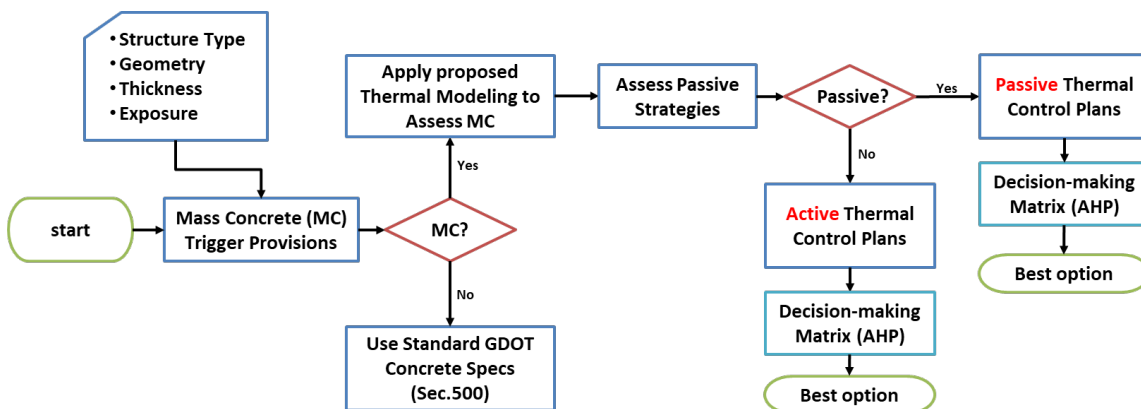


Figure 27. Decision-making process for mass concrete cooling

6.2 AHP analysis

The research team applied AHP analysis to select an optimal alternative for the thermal control of mass concrete. The AHP is a mathematical decision-making matrix based on a group's preference (Saaty & Peniwati, 2013). Figure 28 describes a framework for the AHP structured in this research.

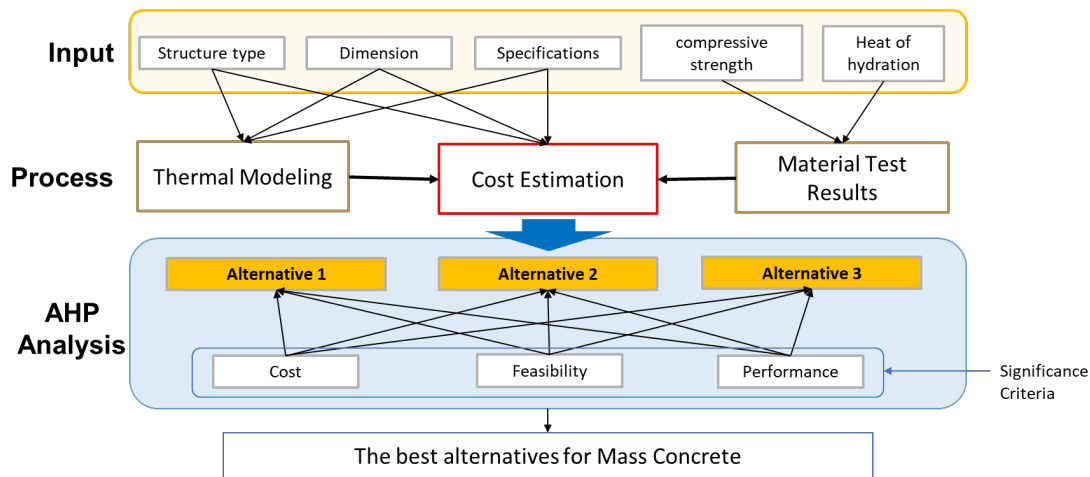


Figure 28. Framework for the AHP

To determine the weights of the criteria, the research team conducted a nationwide online survey to contractors and DOT engineers. The definitions of each criterion are as follows:

- **Cost:** Total of the direct and indirect cost of implementing a cooling method, including materials, labor, and delivery
- **Performance:** The quality and mechanical properties of the cooled mass concrete structures (e.g., in passive strategy, the performance is calculated as compressive strength/heat of hydration)
- **Feasibility:** Constructability for implementing cooling methods, or the availability of material in an area, or the acceptability of cooling methods

The details of the survey are contained in Appendix A. A total of 17 responses were used, excluding outliers. Since there was no significant difference between the owners' (GDOT engineers') answers and the contractors' answers, they were counted together. The AHP can be divided into three consecutive stages:

1. Computation of the vector of criteria weights and consistency
2. Computation of the scores of alternatives
3. Determination of the ranking

To calculate the weights for the criteria, the AHP generates a pairwise comparison matrix, which is a 3×3 matrix as shown in Table 3. Each value of the pairwise comparison matrix represents a significance of each criterion relative to the other criteria. For example, in this study, cost is 1.06 times more important than feasibility (Table 3).

Table 3. The pairwise comparison matrix (3×3) for the criteria

	Cost	Performance	Feasibility
Cost	1.00	0.88	1.06
Performance	1.13	1.00	1.66
Feasibility	0.94	0.60	1.00
Sum	3.08	2.48	3.72

After generating the pairwise comparison matrix, the values in the matrix are normalized with the sum of the values on each column. Finally, the weight vector of each criterion is computed by averaging the values on each rows of the normalized matrix. Table 4 shows the normalized matrix and the importance weight.

Table 4. The normalized matrix (3×3) and the weight vector

	Cost	Performance	Feasibility	Importance weight
Cost	0.325	0.355	0.285	0.322
Performance	0.368	0.403	0.447	0.406
Feasibility	0.307	0.242	0.269	0.273

In AHP, if the consistency ratio (CR), which is an indicator of how consistent the opinions are, is 0.1 or less, it is acceptable to continue the AHP analysis (Saaty, 2005). In this study, as the consistency ratio (CR) is 0.01016, the importance weight is acceptable. With the importance weight, the research team conducted AHP for two scenarios: 1) passive cooling strategy and 2) active cooling strategy. The purpose of the following sections is to provide an example of the AHP for the passive cooling scenario. Since the cost and availability of cementitious materials vary widely by region, the results of the AHP analysis may vary from site to site.

6.2.1 AHP for passive cooling strategies (scenario 1)

In this section, the research team conducted the AHP analysis on a passive cooling scenario to provide an example. For this, the research team collected the cost information of the six mix designs for mass concrete proposed in this study. Table 5 shows the cost information collected from a ready-mixed concrete supplier in Georgia.

Table 5. Cost information of the mix designs proposed in this study

	Baseline	45% FA	25% FA	FA+BFS	Coarse cement	Limestone
Unit price (\$/cy.)	136	134	135	132	134	134

In the passive strategy, the performance is determined by the ratio of the increasing rate of the compressive strength to the increasing rate of the heat generation of the proposed mix designs based on the baseline concrete. See the equation below.

$$\text{Performance} = \frac{\Delta S}{\Delta T}$$

where ΔS is the ratio of the compressive strength of a mixed concrete to that of baseline concrete, and ΔT is the ratio of the hydration heat of a mixed concrete to that of baseline concrete. Their compressive strength and hydration heat were derived from the experiment results in Task 1 (see Figures 8 and 10). In this scenario, as the research team assumed that all materials were equally available, the feasibility scores are equal to 1.0. The results of the AHP analysis are shown in Table 6.

Table 6. AHP results for passive strategies

Mix designs	Cost	Performance	Feasibility	Total score
45% FA	0.33	0.31	0.27	0.91
25% FA	0.32	0.28	0.27	0.88
FA+BFS	0.33	0.47	0.27	1.07
Coarse cement	0.33	0.42	0.27	1.02
Limestone	0.33	0.27	0.27	0.87

In this scenario, FA+BFS concrete was selected as an optimal mixture for the passive cooling strategy for mass concrete because it showed the highest performance. However,

the feasibility scores could be measured differently, because several ready-mix concrete suppliers do not deal with some specific types of admixture. Moreover, since the delivery fee should be different depending on the presence of the admixture, the cost scores could also vary.

7. Conclusion

To summarize, this research was conducted with the series of four tasks. In Task 1, the research team reviewed manuals and specifications for mass concrete in various states. The mass concrete specifications varied depending on the area or the time of establishment. In particular, Florida DOT lists a maximum temperature of 180°F. This is because the Florida DOT has not approved a concrete mixture to be used for mass concrete applications without slag or fly ash. Florida DOT suggests a minimum fly ash content of 25% for all mass concrete, and it is proposed for GDOT to provide the same specification. Based on the literature review, in Task 2, the research team developed five mass concrete mix designs – 45% FA, 25% FA, FA+BFS, coarse cement, and limestone – and conducted comparative experiments with a baseline mix (GDOT AA+ concrete). As a result, the 25% FA mix demonstrates the modest reduction in the peak heat of hydration with good early strength gain. The 45% FA mix demonstrates a significant reduction in the peak heat of hydration, but with a significant delay in strength gain. From the results, the project team recommends that GDOT consider applying the 45% FA mix to the structural elements such as foundations, pile caps, and piers that will not be subject to early loading.

The research team also conducted mid-scale experiments with and without a cooling system and compared the experimental results to the simulation results in Task 3. From the comparative analysis, the research team found that while peak temperatures can be accurately predicted, the rates of heating and passive cooling tend to be under-estimated. Also, the rates of active cooling are slightly over-estimated in this study. The model used to estimate energy release due to hydration was taken from the literature and involves

equations regressed on calorimetry data that provide parameters for an Arrhenius equation. These equations require many inputs, including cement chemistry, some of which are difficult to determine. The resulting uncertainty suggests this as a possible source of under-estimation of heating. Therefore, the future work may include a simplified experimental procedure, possibly amenable to field use, to determine a model for the exothermic nature of hydration. Under-estimation of passive cooling is likely related to inaccurate boundary conditions such as convection coefficients. The over-estimation of active cooling is comparatively lower and may be due to idealizations used in order to model active cooling in a one-dimensional computational model and the empirical relations used to estimate heat transfer relations from water temperatures, material properties, and flow rates. Other future work would include a continuing examination of scaling relations to inform a more precise definition of mass concrete and consideration of practical engineering aids such as general graphical computations to estimate peak temperatures and evaluate methods for thermal control of mass concrete.

In Task 4, the research team developed a decision-making framework for mass concrete construction. The framework first determines whether to apply the mass concrete provision to the target structures based on their dimension and type. If the structures are determined to be mass concrete, the framework decides between passive strategy and active strategy for mass concrete thermal control. After that, the framework finally selects an optimal method via AHP analysis. From the results of a nationwide online survey, the research team determined the importance weights for three criteria – cost, performance, and feasibility – as 0.322, 0.406, and 0.273, respectively. With the importance weights, the

research team carried out AHP to demonstrate it as an example. The results demonstrated that FA+BFS concrete was the best alternative for passive thermal control. However, since the prices and availability of the concrete mixtures depend on the region, the results may vary from region to region.

In this study, all the tests and analyses were conducted under controlled lab environments and simulated situations. Thus, for the future work, it is necessary to validate the mass concrete thermal management methods (e.g., passive or active cooling) and decision-making tools developed from this study through real-world mass concrete construction projects as pilot case studies. Also, the real-world cost implication of thermal management methods needs to be investigated.

REFERENCES

1. Al-Manaseer, A., & Elias, N. (2008). *Placement of mass concrete for cast-in-place concrete piling: the effects of heat of hydration of mass concrete for cast-in-place piles*. California. Dept. of Transportation. Division of Research and Innovation.
2. ASTM. (2017). Standard Practice for Accelerated Curing of Concrete Cylinders. In *Astm Standards* (pp. 1–6). West Conshohocken, PA.: ASTM International.
3. Chini, A. R., Muszynski, L. C., Acquaye, L., & Tarkhan, S. (2003). *Determination of the Maximum Placement and Curing Temperatures in Mass Concrete to Avoid Durability Problems and DEF*.
4. Eiland, A. (2016). *Development of Specifications for ALDOT Mass Concrete Construction*. Auburn University.
5. FDOT. (2015). Specifications for limerock base and stabilized base materials. *Road and Bridge Construction Manual*, (Section 911).
6. Gajda, J., & Vangeem, M. (2002). Controlling temperatures in mass concrete. *Concrete International*, 24(1), 58–62.
7. Georgia Department of Transportation. (2006). Section 500 - Concrete Structures. In *DEPARTMENT OF TRANSPORTATION STATE OF GEORGIA SUPPLEMENTAL SPECIFICATION*.
8. Georgia Department of Transportation. (2013). Section 500 - Concrete Structures. In *DEPARTMENT OF TRANSPORTATION STATE OF GEORGIA SPECIAL PROVISION*.
9. Mindeguia, J. C., Pimienta, P., Noumowé, A., & Kanema, M. (2010). Temperature, pore pressure and mass variation of concrete subjected to high temperature -

Experimental and numerical discussion on spalling risk. *Cement and Concrete Research*, 40(3), 477–487.

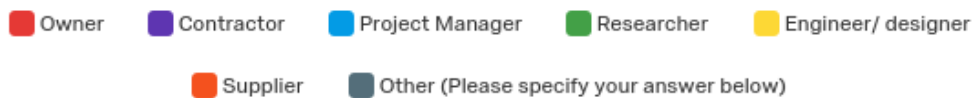
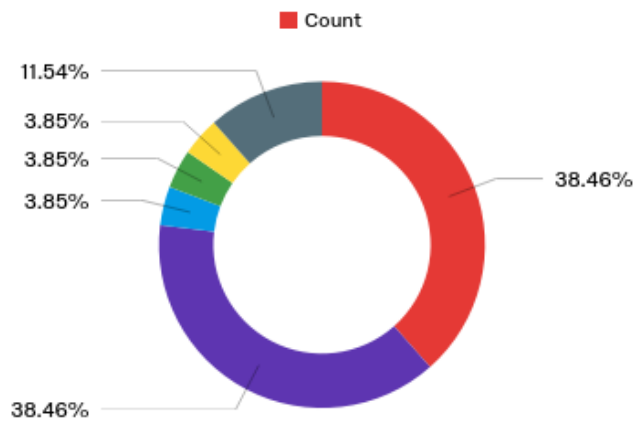
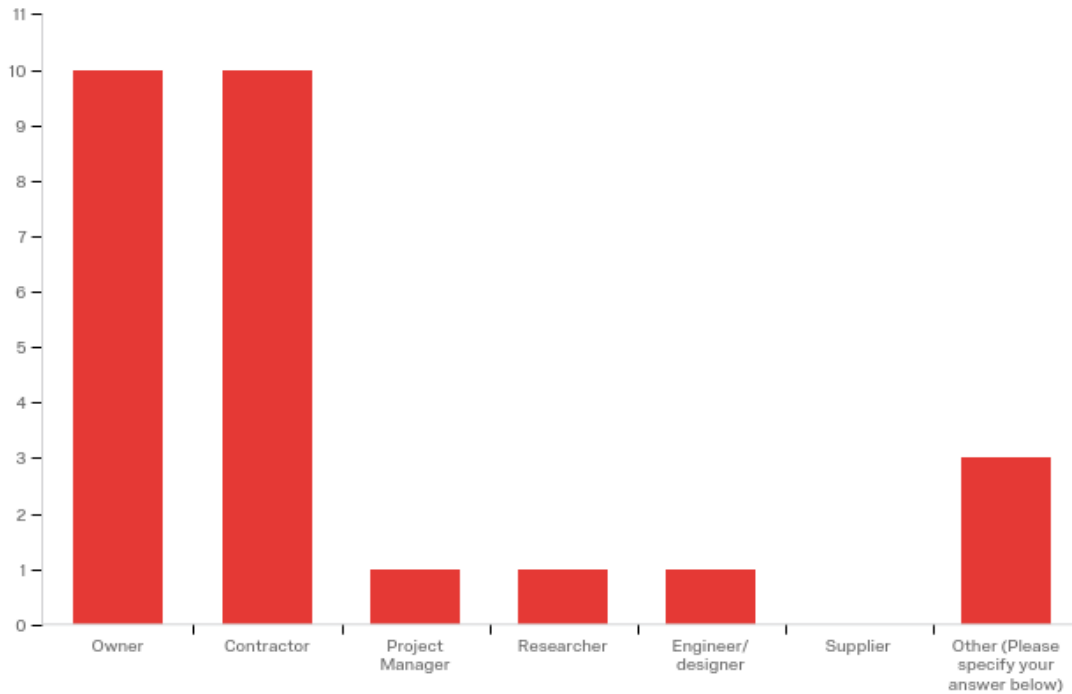
10. Riding, K. A., Poole, J. L., Folliard, K. J., Juenger, M. C. G., & Schindler, A. K. (2012). Modeling hydration of cementitious systems. *ACI Materials Journal*, 109(2), 225–234.
11. Riding, K. A., Poole, J. L., Schindler, A. K., Juenger, M. C. G., & Folliard, K. J. (2006). Evaluation of temperature prediction methods for mass concrete members. *ACI Materials Journal*, 103(5), 357–365.
12. Saaty, T. L. (2005). *Decision making for leaders: the analytic hierarchy process for decisions in a complex world*. RWS publications.
13. Saaty, T. L., & Peniwati, K. (2013). *Group decision making: drawing out and reconciling differences*. RWS publications.
14. Schindler, A. K., & Folliard, K. J. (2005). Heat of Hydration Models for Cementitious Materials. *Materials Journal*, 102(1).

Appendix A

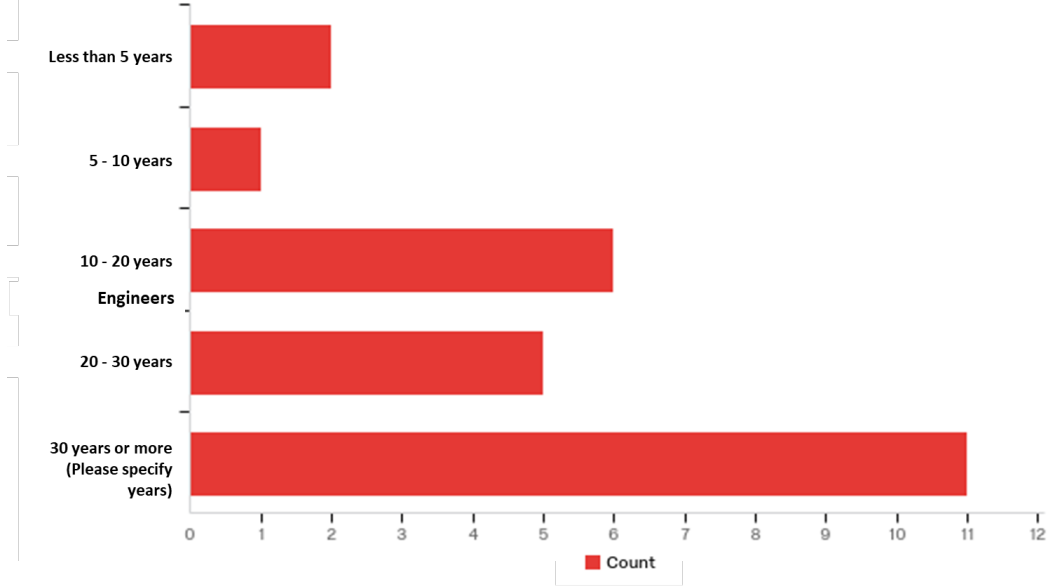
Survey Report

mass concrete cooling methods

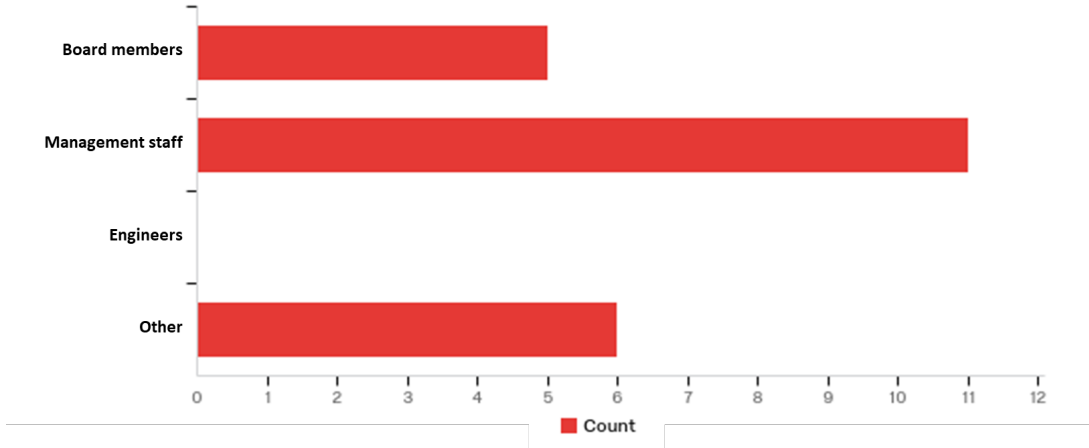
Q1. In what category do you belong?



Q2. How long have you worked in the roadway construction field?

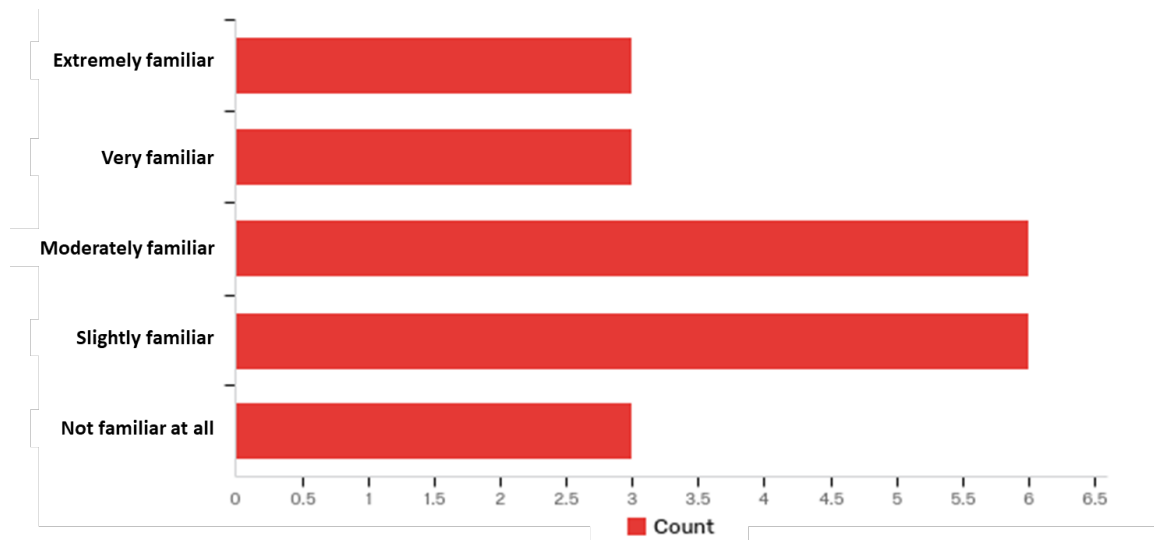


Q3. Please identify your position with your employer.

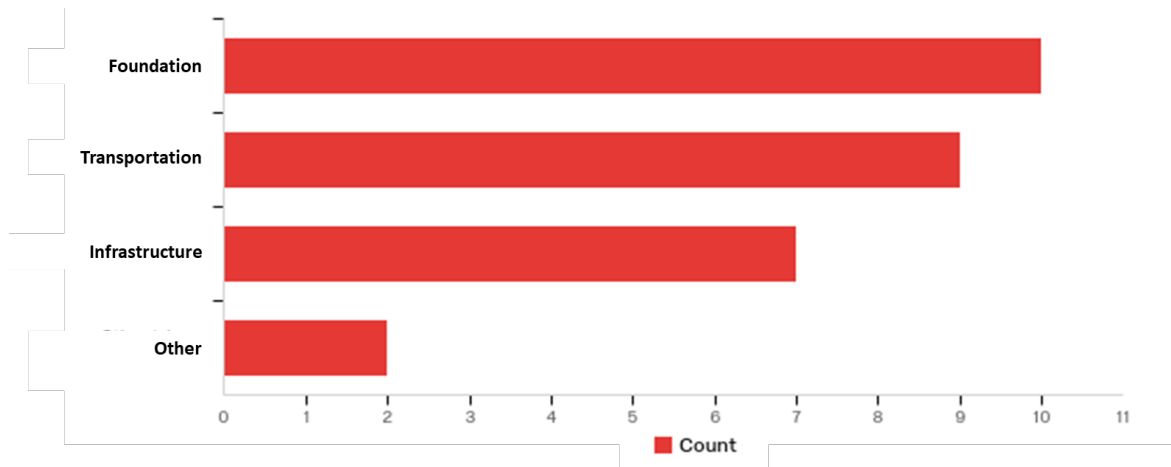


Other answers	%	Count
Not available	16.67%	1
Owner/ CEO	16.67%	1
President	16.67%	1
Undergraduate Researcher	16.67%	1
Vice President	16.67%	1
Vice President/Project Manager	16.67%	1
Total	100%	6

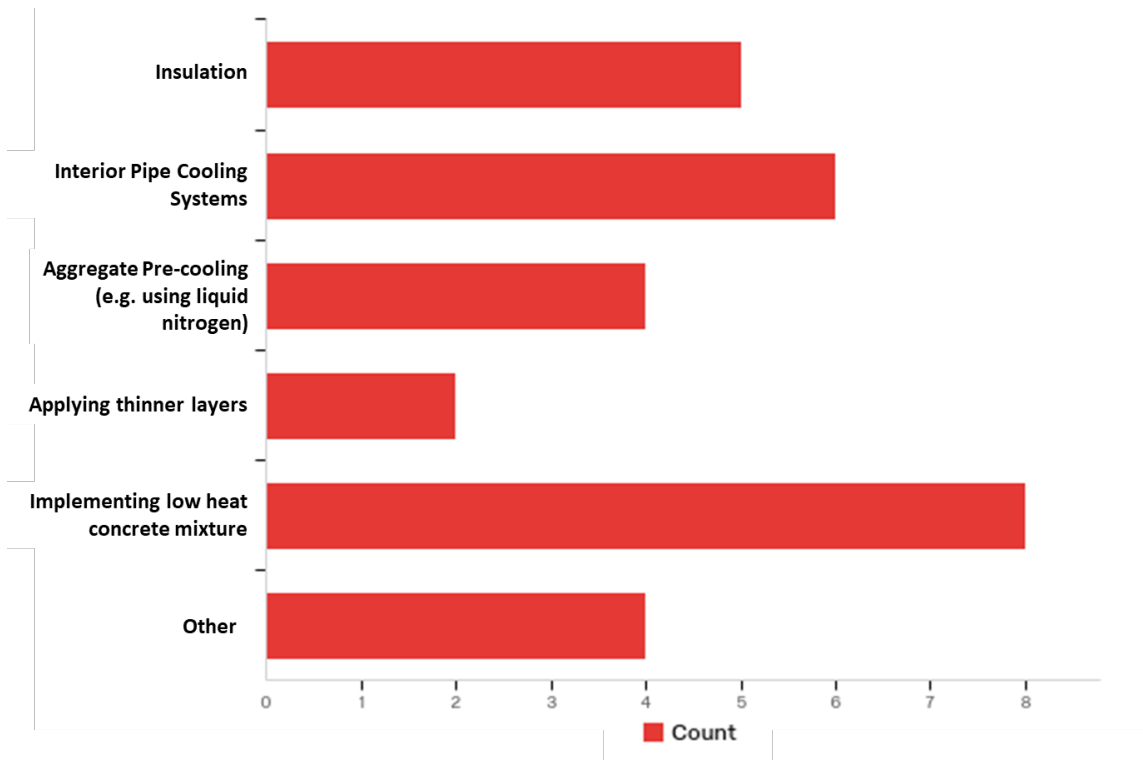
Q4. How familiar are you with mass concrete projects?



Q5. What type of mass concrete project were you working on? (Select all)



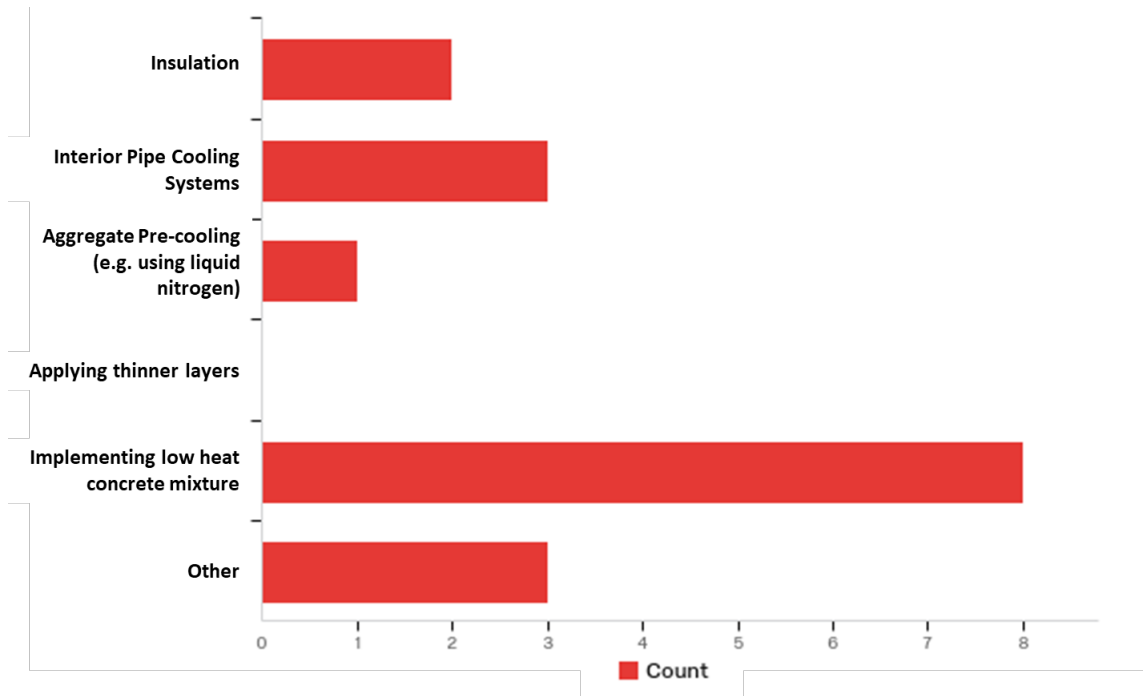
**Q6. Which mass concrete cooling method has your project implemented?
(Select all)**



Other answers

<ul style="list-style-type: none"> • White membrane curing
<ul style="list-style-type: none"> • Add ice to mix
<ul style="list-style-type: none"> • Add ice to mix
<ul style="list-style-type: none"> • Concrete curing compound and plastic sheeting to keep the moisture from evaporating

Q7. From your experience, what do you think is the most efficient method to control hydration heat in mass concrete projects?



Questions for AHP

Q8 – Q11. A is (___) time(s) as important as B.

Subject #	Cost vs. Performance	Cost vs. Feasibility	Performance vs. Feasibility
1	0.5	0.5	2
2	2	1	3
3	0.5	2	2
4	1	2	1
5	0	0	3
6	1.5	2	1.5
7	1	0.5	2
8	1	1	1.5
9	0.5	0.5	1
10	0	0	2
11	0.5	0.5	0.5
12	2	2	2
13	0.5	1	2
14	0.5	0.5	1
15	0	2	2
16	0.5	0.5	1
17	3	2	0.75
Sum:	15	18	28.25
Average:	0.882	1.059	1.662